Chapter 20
HSP90 Inhibitors Blocking Multiple Oncogenic Signaling Pathways for the Treatment of Cancer

Fen Jiang, Xiao-Li Xu, and Qi-Dong You

Abstract Heat shock protein 90 (HSP90) is an ATP-dependent molecular chaperone which plays important roles in the development of cancer. Inhibition of the HSP90 chaperone function can disrupt multiple cancer dependent signaling pathways and result in potent anti-cancer effects, which has been a promising anti-cancer strategy. Up to now, HSP90 inhibitors with different mechanisms have been developed, including HSP90 N-terminal inhibitors (pan-isoform and isoform selective), C-terminal inhibitors and HSP90-cochaperone protein-protein interaction (PPI) inhibitors. In this chapter, we will review the current development of HSP90 inhibitors as anti-cancer agents.

Keywords Cancer · GRP94 · HSP90-CDC37 PPI · HSP90 inhibitor · Isoform selective · TRAP1

Abbreviations

BTZ	bortezomib
CR	complete response
CTD	C-terminal domain
DHPM	3,4-dihydropyrimidin-2-(1H)-one
DLTs	dose-limiting toxicities
EGCG	epigallocatechin gallate
ER	endoplasmic reticulum
ESCC	esophageal squamous cell carcinoma
FU	5-fluorouracil
GRP94	glucose-regulated protein 94

F. Jiang · X.-L. Xu · Q.-D. You (✉)
State Key Laboratory of Natural Medicines and Jiang Su Key Laboratory of Drug Design and Optimization and Department of Medicinal Chemistry, School of Pharmacy, China Pharmaceutical University, Nanjing, China
e-mail: youqd@cpu.edu.cn

A. A. A. Asea, P. Kaur (eds.), *Heat Shock Proteins in Signaling Pathways*, Heat Shock Proteins 17, https://doi.org/10.1007/978-3-030-03952-3_20

HGF	hepatocyte growth factor
HSP	Heat shock protein
HTRF	homogeneous time-resolved fluorescence
IGFs	insulin-like growth factors
IRI	irinotecan
l-OHP	oxaliplatin
MD	middle-domain
MM	multiple myeloma
MTD	maximum tolerance dose
NSCLC	non-small cell lung cancer
NTD	N-terminal domain
PPI	protein-protein interaction
PR	partial response
RDA	radamide
SD	stable disease
SDH	succinate dehydrogenase
SPR	surface plasmon resonance
TEAEs	treatment-related adverse events
TRAIL	TNF-α–related apoptosis-inducing ligand
TRAMP	transgenic adenocarcinoma of the mouse prostate
TRAP1	tumor necrosis factor receptor-associated protein-1

20.1 Introduction

Heat shock proteins (HSP) are molecular chaperones that are curial for the maturation, stability and function of other proteins named “client proteins”. Hsp include large Hsp, HSP90, HSP70, HSP60, HSP40 and small HSP. Among which, HSP90 is the most well studied one in the last decades (Garcia-Carbonero et al. 2013). As the most abundant intracellular protein in mammalian cells, HSP90 comprises approximately 1–2% of total cell protein under normal conditions. While under stressed conditions (heat, hypoxia and nutrient deprivation), HSP90 is upregulated to maintain the cellular homeostasis (Barrott and Haystead 2013). There are four HSP90 isoforms in higher eukaryotes, cytosolic HSP90α and HSP90β, endoplasmic reticulum (ER) paralog glucose-regulated protein 94 (GRP94) and mitochondria paralog tumor necrosis factor receptor-associated protein-1 (TRAP1). Despite the high homologies, the four isoforms possess different cellular functions and have different client profiles (Gewirth 2016). In mammalian cells, HSP90 exists as a homodimer, and each monomer is consisted of three domains: N-terminal domain (NTD), middle-domain (MD), and C-terminal domain (CTD). The NTD incorporates an ATP binding site, which hydrolyzes ATP to provide energy for the chaperone function. The MD provides binding sites for clients and cochaperones. The CTD is important for the dimerization. Recent studies suggest that another ATP

binding pocket is located at CTD (Miyata et al. 2013). The chaperone function of HSP90 relies on an ATP triggered chaperone cycle. ATP binding leads to transient dimerization of the NTD, then several cochaperones (CDC37, HSP70, P23, HOP, etc.) form a chaperone complex with HSP90 to regulate the folding and release of the client proteins (Calderwood 2013). HSP90 plays important roles in the development of cancer, and HSP90 inhibition is proved to be a promising anti-cancer strategy. To data, HSP90 inhibitors with different mechanisms have been developed, including HSP90 N-terminal inhibitors, C-terminal inhibitors and inhibitors blocking the PPI between HSP90 and cochaperones. These inhibitors block multiple cancer dependent signal pathways and exhibit potent pre-clinical anti-cancer effects both in vitro and in vivo. Moreover, several HSP90 N-terminal inhibitors have entered clinical trails. In this chapter, we will review the development progress of HSP90 inhibitors as anti-cancer agents.

20.2 HSP90 and Cancer

HSP90 is reported to be over-expressed in tumors two to threefold higher than corresponding non-tumorigenic tissue (Barrott and Haystead 2013). Cancer cells are addictive to the HSP90 chaperone function to prevent the mutated and overexpressed oncoproteins from degradation (Trepel et al. 2010). Among the over 500 client proteins of HSP90 (https://www.picard.ch/downloads/Hsp90interactors.pdf.), many are notorious oncogenic proteins, including tyrosine-kinase receptors (EGFR, HER2, SRC, MEK, etc.), signal-transduction proteins (BCR-ABL, ALK, BRAF, AKT, etc.), transcription factors (AR, OR, HIF1α, P53, etc.), cyclin-dependent proteins (CDK4, CDK6, Cyclin D, etc.), antiapoptotic proteins (BCL2, Survivin), matrix metalloproteinases (MMP-2, MMP-9) and telomerase (hTERT) (Garcia-Carbonero et al. 2013; Verma et al. 2016). These oncogenic client proteins are involved in multiple cancer dependent signaling pathways.

GRP94 is the ER paralog of HSP90. Clinically, high expression of GRP94 is associated with the advanced stage and poor prognosis of some types of carcinomas, including hepatocellular carcinoma, multiple myeloma, gallbladder cancer, et al. (Chen et al. 2015; Chhabra et al. 2015; Rachidi et al. 2015). GRP94 has a limited client protein profile, and some client proteins correlate with the development and metastasis of cancer. Integrins are a major class of GRP94 client proteins. They mediate cell–cell, cell–extracellular matrix communication and are important for cell adhesion and metastasis (Desgrosellier and Cheresh 2010). GRP94 based α-helix peptide blocking the interaction between GRP94 and integrins inhibited cell invasion (Hong et al. 2013). In addition, GRP94 knockdown led to reduce migration and metastasis potential of MDA-MB-231 cells and ROS resistant MCF-7 cells (Dejeans et al. 2012). The maturation and secretion of Insulin-like growth factors (IGFs) are also dependent on GRP94 (Barton et al. 2012; Marzec et al. 2016; Ostrovsky et al. 2009; Wanderling et al. 2007). Both IGF1 and IGF2 play important

roles in cancer, and IGF pathway inhibition has been considered as a novel anti-cancer strategy (Brahmkhatri et al. 2015; King and Wong 2016). Bei Liu and coworkers discovered that GRP94 bound and promoted the exportation of Wnt coreceptor LRP6 from ER to cell surface (Liu et al. 2013). Their further study demonstrated that GRP94 deficiency blocked Wnt-LRP-Survivin pathway in human multiple myeloma cells, and induced cell apoptosis and tumor growth inhibition in xenograft models (Hua et al. 2013). Recent studies showed that surface GRP94 interacted with HER2 and facilitated HER2 dimerization. Purine-scaffold GRP94 specific inhibitor **PU-WS13**, GRP94 based α-helix peptide or anti-GRP94 monoclonal antibody treatment led to decreased HER2 level in SKBr3 cells and exhibited selective therapeutic effects in HER2 positive breast cancers (Li et al. 2015a, b; Patel et al. 2013, 2015).

TRAP1, the mitochondrial paralogue of HSP90, is also reported to be elevated in various human carcinomas, including colorectal carcinoma, prostate cancer, ovarian carcinoma, breast cancer, non-small cell lung cancer (NSCLC) and esophageal squamous cell carcinoma (ESCC). The high TRAP1 expression is associated with the progress and prognostic of these carcinomas (Agorreta et al. 2014; Costantino et al. 2009; Landriscina et al. 2010; Leav et al. 2010; Maddalena et al. 2013; Tian et al. 2014). TRAP1 is involved in the proliferation and apoptosis of cancer cells. In ESCC cells, knockdown of TRAP1 inhibited the proliferation, induced cell cycle arrest and apoptosis. While re-expression of TRAP1 promoted cell proliferation and reduced cell apoptosis (Tian et al. 2014). TRAP1 also promoted neoplastic growth by binding and inhibiting succinate dehydrogenase (SDH). TRAP1 dependent SDH inhibition led to respiratory down-regulation and succinate accumulation. Succinate then stabilized HIF-1α and prompted neoplastic growth (Sciacovelli et al. 2013). Studies in Matteo Landriscina group suggested that TRAP1 was involved in drug resistance of cancer cells. TRAP1 up-regulation was observed in HT-29 colorectal carcinoma cells resistant to 5-fluorouracil (FU), oxaliplatin (l-OHP) and irinotecan (IRI), and was responsible for the multi-drug resistance (Costantino et al. 2009). As the mitochondrial paralogue of HSP90, TRAP1 was also demonstrated locating in ER and involving in ER stress protection and protein quality control of tumor cells. The ER-associated TRAP1 protected MCF7 and MBA-MB-231 cells from paclitaxel-induced apoptosis and was relevant in paclitaxel resistance of these breast carcinoma cells (Maddalena et al. 2013). ER-associated TRAP1 was also responsible for the anthracyclins resistance of breast carcinoma cells (Sisinni et al. 2014). In general, HSP90 isoforms are involved in multiple cancer dependent signaling pathways. HSP90 inhibition is a promising anti-cancer strategy.

20.3 HSP90 N-Terminal Inhibitors

Inhibitors competitively occupy the NTD ATP binding pocket can block the HSP90 chaperone function. These inhibitors are named HSP90 N-terminal inhibitors.

20.3.1 Pan-HSP90 N-Terminal Inhibitors

Up to now, more than 20 distinct N-terminal HSP90 inhibitors have entered clinical trails. These are pan-HSP90 inhibitors that exhibit similar affinities to the four isoforms. As shown in Fig. 20.1, these inhibitors can be divided into three classes. Geldanamycin analogues are the first-generation inhibitors, including **17-AAG**, **17-DMAG**, **IPI-493** and **IPI-504**. To solve the unfavorable drug-like properties of the geldanamycin analogues, the second-generation synthetic small molecule inhibitors are developed, including purine derivatives, resorcinol derivatives and benzamide derivatives. The pre-clinical properties and clinical performance of these inhibitors have been thoroughly reviewed. Despite the favorable pre-clinical anti-tumor activity, all these inhibitors exhibit poor clinical efficacy in mono-therapy. Some inhibitors only show moderate anti-cancer effects in specific cancer types when combined with other anti-cancer agents. In 2015, the highly anticipated phase III study of **STA-9090** combined with docetaxel for the treatment of advanced stage lung adenocarcinoma was failed. The **STA-9090** and docetaxel combination regimen did not result in improved efficacy compared with docetaxel mono-therapy. In clinical trials, these inhibitors exhibited many treatment-related adverse events (TEAEs). The

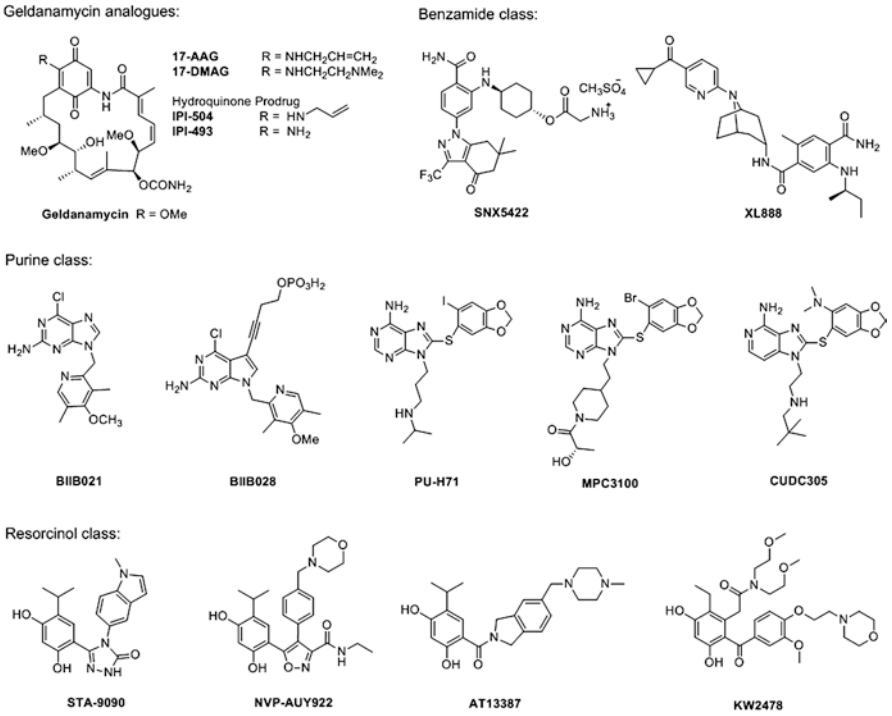

Fig. 20.1 Structures of representative pan-HSP90 N-terminal inhibitors

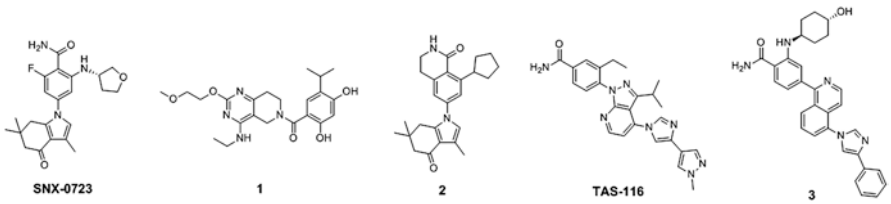

Fig. 20.2 Structures of HSP90α/β selective inhibitors

most common side effects were fatigue, visual disorders, gastrointestinal disorders (nausea, vomiting and diarrhoea), anaemia and neutropenia (Bhat et al. 2014b; Biamonte et al. 2010; Garcia-Carbonero et al. 2013). Because of the disappointing clinical performance, the clinical studies of most inhibitors are terminated. Now, only the resorcinol derivative **AT-13387** and the benzamide derivative **XL888** are active in clinical trials (Fig. 20.2).

The disappointing clinical performance of these pan-HSP90 N-terminal inhibitors can be partly attributed to the following reasons. (1) The clinical dosages of these inhibitors are limited because of the various adverse events, which lead to the drug exposure levels in patients are insufficient to effectively inhibit tumor cell HSP90. HSP90 four isoforms have different functions and chaperone different client proteins. Pan-HSP90 N-terminal inhibitors inhibit the four isoforms simultaneously, which may lead to mechanism related adverse events. Thus, isoform selective HSP90 N-terminal inhibitors may reduce the adverse events and improve the clinical performance. (2) The pan-HSP90 inhibitors trigger significant heat shock response. The increased cytoprotective HSP (HSP70 and HSP27) partly neutralize the anti-cancer effects. Studies have shown that GRP94 selective inhibitors, TRAP1 selective inhibitors and HSP90 C-terminal inhibitors don't induce heat shock response. These inhibitors may have more promising usage as anti-cancer agents.

20.3.2 Isoform Selective HSP90 N-Terminal Inhibitors

HSP90 isoform selective inhibitors only influence partial isoform specific client proteins. Theoretically, isoform selective inhibitors will have reduced adverse effects compared with the pan-inhibitors. In addition, GRP94 selective inhibitors and TRAP1 selective inhibitors don't induce heat shock response. Though isoform selective inhibition is attractive, it used to be considered very difficult. HSP90 four isoforms are highly homologous. HSP90α possess 93%, 59%, and 47% sequence similarity with HSP90β, GRP94, and TRAP1, respectively. Even worse, the residues in ATP-binding pocket are more heavily conserved (Ernst et al. 2014a). However, isoform selective inhibitors have been developed recently. The isoform selective inhibition can be attributed to the conformation flexibility of the HSP90 ATP-binding pocket.

20.3.2.1 HSP90α/β Selective Inhibitors

Some HSP90 inhibitors exhibit moderate selectivity for the cytosolic HSP90α/β, such as the benzamide-based **SNX2112** and purine-based **BIIB021**. While some other inhibitors exhibit no selectivity, such as the resorcinol-based **NVP-AUY922**. As the paralogue of **SNX2112**, **SNX0723** exhibits similar HSP90α/β selectivity with **SNX2112**. It was used as the probe molecule to analyze the structural basis for the HSP90α/β selective inhibition. In **SNX0723** bound HSP90α (Fig. 20.3b), the hydrophobic tetrahydroindolone moiety targeted into the big hydrophobic pocket (Site 1) formed by Leu107, Ile110, Ala111, Phe138, Tyr139 and Trp162. To accommodate this binding mode, the flexible loop sequence 104–111 was induced to form an extended α-helix conformation with the H3 and H4 helix. The residues Leu107, Ile110 and Ala111 covered on the tetrahydroindolone moiety and formed hydrophobic interactions with it. In **SNX0723** bound GRP94 (Fig. 20.3c), the equivalent sequence of HSP90α 104–111 in GRP94 (160–167) were disordered. The hydrophobic interactions between tetrahydroindolone moiety and the equivalent residues of Leu107, Ile110, Ala111 in GRP94 were missing, which led to the lower affinity to GRP94 compared with HSP90α/β. The different ligand-bound conformations of HSP90α/β and GRP94 can be attributed to the minimal primary sequence difference. Compared with HSP90α/β, five amino acids (QEDGQ) are inserted in GRP94 at position 126 (HSP90α numbering). For TRAP-1, two amino acid (AE) are inserted at position 129. The amino acid insertions are unfavorable for the ligand induced extended α-helix conformation. The pan-HSP90 inhibitors (such as **NVP-AUY922**, Fig. 20.3a) can't induce the extended α-helix conformation, so they exhibit no discrimination for the four isoforms (Ernst et al. 2014a; Gewirth 2016). Compound **1** developed in our lab could conduct both flexible loop conformation and extended α-helix conformation to bind with HSP90α, so **1** possessed moderate HSP90α selective inhibition against GRP94 (Jiang et al. 2016b). These analyses

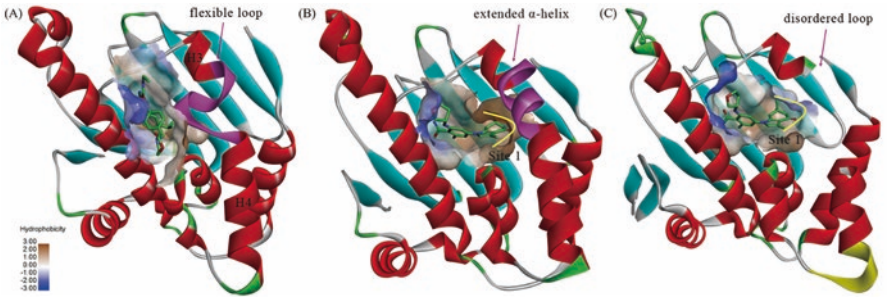

Fig. 20.3 Structural insights of the HSP90α/β selective inhibition. (**a**) NVP-AUY922 bound HSP90α (PDB ID: 2VCI), the flexible loop sequence 104–111 is colored in magenta. (**b**) SNX0723 bound HSP90α (PDB ID: 4NH8), the sequence 104–111 on the extended α-helix is colored in magenta. (**c**) SNX0723 bound GRP94 (PDB ID: 4NH9), the inserted five amino acids (QEDGQ) are colored in yellow. Carbon atoms of the compounds are shown in green. The active sites of the proteins are surfaced according to the hydrophobic state

provide structural insights for the design of inhibitors with improved HSP90α/β selectivity.

Inspired by the above analyses, researchers in Vertex Pharmaceuticals conducted extensive SAR study focused on **SNX0723** to discover more potent and selective HSP90α/β inhibitors. Structure optimization led to cyclopentyl analogue **2**, which exhibited improved HSP90α/β selective inhibition activity, with Ki value of 5 nM for HSP90α/β and >10 μM for GRP94 and TRAP1. In human HD patient derived fibroblasts, **2** induced significant up-regulation of HSP70 and degradation of the HSP90α/β clients htt, CDK4 and AKT (Ernst et al. 2014b). The goal of this research was to develop HSP90α/β selective inhibitors for the treatment of CNS disorders, so the anti-cancer effects of **2** were not evaluated. Considering the significant oncogenic clients degradation effects and the HSP90α/β addiction of tumor cells, **2** should have potent anti-cancer effects.

TAS-116 is another HSP90α/β selective inhibitor which has already entered clinical trials. This compound was developed by Taiho Pharmaceutical Co. LTD. through fragment based drug design. **TAS-116** possessed excellent HSP90α/β selective inhibition activity with Ki values of 34.7 nM, 21.3 nM, >50 μM, and >50 μM for HSP90α, HSP90β, GRP94, and TRAP1, respectively (Ohkubo et al. 2015). The accurate binding mode of **TAS-116** was not reported, while the crystal structure of **TAS-116** homolog **3** complexed with HSP90α was released. Considering the similar structure of the two compounds, **TAS-116** and compound **3** should take same binding modes. As shown in Fig. 20.4, compound **3** also induced an extended α-helix conformation. In addition to the Site 1 pocket, **3** also targeted into a specific hydrophobic pocket (Site 4) which extended toward the opposite side of the ATP pocket. The excellent HSP90α/β selective inhibition could be partially attributed to the occupation of this pocket (Ohkubo et al. 2012).

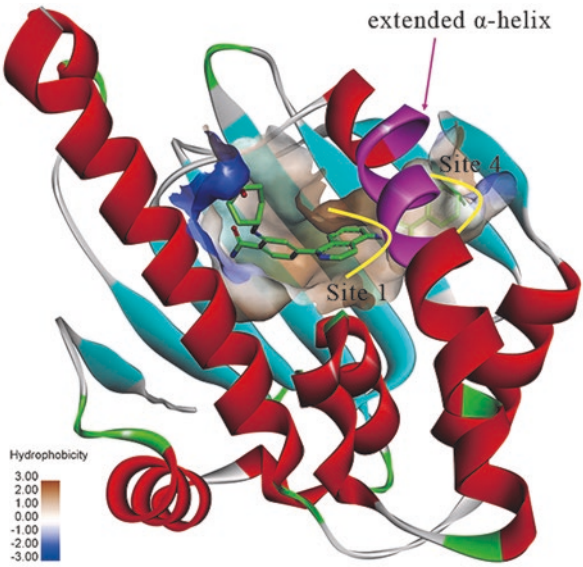

Fig. 20.4 Binding mode analysis of compound 3 complexed with HSP90α (PDB ID: 3WQ9). The sequence 104–111 on the extended α-helix is colored in magenta. Carbon atoms of the compounds are shown in green. The active sites of the proteins are surfaced according to the hydrophobic state

The specific HSP90α/β inhibition of **TAS-116** was confirmed at cellular level. In HCT116 cells, **TAS-116** treatment induced the degradation of DDR1 (client of HSP90α) and the up-regulation of HSP70, while exhibited no influence on the LRP6/GRP94 complex formation and LRP6 expression level (LRP6 is the client of GRP94). In pre-clinical study, oral administration of **TAS-116** exhibited potent anti-tumor activity in various xenograft models. In HER2-expressing NCI-N87 human gastric cancer xenografts, **TAS-116** inhibited tumor growth significantly in a dose dependent manner. The T/C value was 47%, 21%, and 9% for dose of 3.6 mg/kg, 7.1 mg/kg, and 14.0 mg/kg, respectively. **TAS-116** treatment downregulated the HSP90 clients HER2, HER3, and AKT in tumor tissues, indicting the potent anti-tumor activity was HSP90 inhibition dependent. As results, the PI3K/AKT and MAPK/ERK signaling pathways were inhibited. In FLT3-ITD-expressing MV-4-11 human acute myeloid leukemia xenografts, 14.0 mg/kg/day **TAS-116** administration led to tumor shrinkage, accompanied with FLT3-ITD degradation in tumors. In an orthotopic lung tumor model expressing EGFR (L858R/T790M), **TAS-116** administration also inhibited tumor growth significantly (Ohkubo et al. 2015).

Multiple myeloma (MM) was reported to be sensitive to HSP90 inhibitors in both pre-clinical models and clinical trails (Kaiser et al. 2010; Patterson et al. 2008; Richardson et al. 2010a, b, 2011; Stuhmer et al. 2008). As a potential therapeutic agent, the pre-clinical anti-MM activity of **TAS-116** alone or in combination with other agents was well studied. **TAS-116** exhibited potent cytotoxicity in a series MM cell lines and patient derived MM cells, including RAS-mutated MM cells (Suzuki et al. 2015a, b). Moreover, **TAS-116** could overcome **17-AAG** resistance mechanisms and was more effective than 17-AAG in N-RAS mutated MM cell lines, associated with lower HSP27 induction and more significant degradation of the clients p-C-RAF and p-MEK1/2. In addition, **TAS-116** augmented the bortezomib (**BTZ**) cytotoxicity against MM cells. The synergistic activity was due to inhibition of **BTZ**-triggered canonical NF-κB activation and enhanced unfolded protein response (UPR). In murine xenografts, both **TAS-116** alone and combination with BTZ exhibited potent anti-MM activities. The combination treatment inhibited tumor growth more potently than **TAS-116** and **BTZ** monotherapy. The OS of combination treated animals was significantly prolonged. (Suzuki et al. 2015a). Considering that **TAS-116** induced significant degradation of key RAS-RAF-MEK-ERK pathway regulators (p-C-RAF, p-MEK1/2, and p-ERK), the synergistic anti-MM activities of **TAS-116** in combination with RAS-RAF-MEK-ERK signaling pathway inhibitors were studied. In RAS mutated MM cell lines, **TAS-116** significantly enhanced the cytotoxicity and apoptosis induction effects of tipifarnib (farnesyltransferase inhibitor), dabrafenib (RAF inhibitor), and **AZD6244** (MEK inhibitor). In B-RAF-mutated U266 MM cell line, synergistic cytotoxicity of **TAS-116** combination with dabrafenib was also observed (Suzuki et al. 2015b). All these results indicting **TAS-116** is a potent anti-MM agent, either alone used or combined with other agents.

As a favorable property, **TAS-116** exhibited no ocular toxicity in pre-clinical study. In human retinal pigment epithelial ARPE-19 cells that were essential for the support of photoreceptors, **TAS-116** was less toxic than **17-AAG** (Suzuki et al.

2015a). In NCI-H1975 rat xenografts, **TAS-116** exhibited low retina exposure and high tumor/retina drug exposure ratio. In addition, administration of **TAS-116** in SD rats didn't induce cell apoptosis and histologic change in the outer nuclear layer of the retina (Ohkubo et al. 2015).

Inspired by the excellent pre-clinical anti-tumor effects and safety profile, **TAS-116** entered clinical trials in 2014 for the phase I dose escalation study enrolled patients with advanced solid tumors. Preliminary clinical data reported in 2015 revealed that two patients (GIST and NSCLC) had partial response (PR) and five patients had stable disease (SD) more than 12 weeks in the qd dose regimen (n = 16) (Shimomura et al. 2015). During the whole study, patients (n = 52) received **TAS-116** according to three dose regimens, were 4.8–150.5, 107.5–295.0 and 160 mg/m^2 day in qd, qod and qd×5, respectively. The maximum tolerance dose (MTD) for qd and qod regimen was 107.5 and 210.7 mg/m^2 day, respectively. Anorexia, AST/ALT/gamma-GTP elevation, night blindness and visual disorders, platelet decrease (grade 3), septic shock, respiratory failure, pneumonia (grade 4) and febrile neutropenia (grade 3) were the observed dose-limiting toxicities (DLTs). For efficacy assessment, in qd, qd×5 and qod groups, PR was achieved by 12.5, 0 and 5.6%; SD was achieved by 43.8, 61.5 and 38.9%; disease control rate (>/=12 weeks) was 31.1%, 46.2% and 22.2%, respectively (Yanagitani et al. 2017). This phase I study revealed the preliminary clinical anti-cancer activity of **TAS-116**. In the further phase II study in patients with GIST (n = 40), **TAS-116** was orally administrated on a 5-days-on/2-days-off schedule. TEAEs were observed in all patients, and 52.5% were grade 3 or higher. Gastrointestinal disorders were the most common TEAEs and could be resolved with dose interruption. Other TEAEs including diarrhea, anorexia, nausea, ALT/AST increase, anemia, fatigue, vomiting, rash and bladder infection. Of the 40 patients enrolled, the median progression-free survival was 4.4 months and no complete response (CR) and PR was achieved. Thirty-four (85%) patients had SD lasting >/= 6 weeks (Kurokawa et al. 2017). Another phase I study is ongoing in US and UK to evaluate the MTD, safety, tolerability and efficacy of **TAS-116** in patients with advanced solid tumors (Takanami 2005). Based on these reported clinical data, though **TAS-116** was well-tolerated, it still manifested many TEAEs. In addition, no significant anti-tumor activity was observed during the treatment. The clinical safety and efficacy of **TAS-116** should be further studied.

20.3.2.2 GRP94 Selective Inhibitors

In consideration of the correlation between GRP94 and cancer, many GRP94 selective inhibitors have been developed and exhibited promising pre-clinical anti-cancer effects. As shown in Fig. 20.5, many GRP94 selective inhibitors have been developed. Same as the pan-HSP90 N-terminal inhibitors, GRP94 selective inhibitors can also be divided into three types. As a typical adenosine receptors agonist, purine scaffold **NECA** was the first discovered GRP94 selective inhibitor. It bound to purified GRP94 with a dissociation constant of 200 nM while exhibited no binding to purified HSP90 (Rosser and Nicchitta 2000). Simple structure modification focused

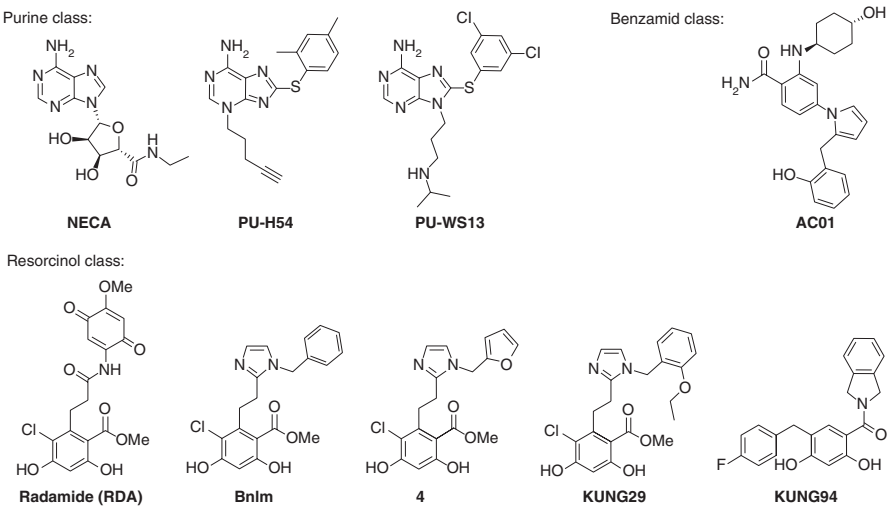

Fig. 20.5 Structures of GRP94 selective inhibitors

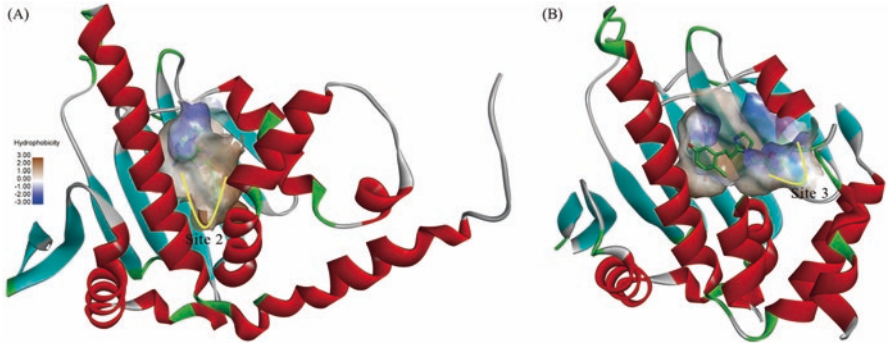

Fig. 20.6 Structural insights of the GRP94 selective inhibition. (**a**) GRP94-PU-H54 complex (PDB ID: 3O2F). (**b**) GRP94-4 complex (PDB ID: 5IN9). Carbon atoms of the compounds are shown in green. The active sites of the proteins are surfaced according to the hydrophobic state

on N-ethyl moiety of **NECA** didn't lead to derivatives with higher binding affinity (Immormino et al. 2009). Considering the off-target adenosine receptor pathway activation effect of the purine scaffold and the limited structure modification feasibility, **NECA** is not a proper lead compound for further development. The cellular GRP94 inhibition effect of **NECA** has not been reported. In 2013, combined compound library screening with structural and computational analyses led to the discovery of another purine scaffold GRP94 selective inhibitor **PU-H54**. As shown in Fig. 20.6a, crystal complex showed that **PU-H54** induced rearrangements of the GRP94 lid region, and occupied the newly exposed hydrophobic Site 2 pocket. Further structure modification led to **PU-WS13**, which exhibited more potent and

selective GRP94 inhibition activity. **PU-WS13** inhibited IGF-II secretion and TLR9 trafficking in cells in a dose dependent manner, and exhibited no effects on HSP70 induction and AKT degradation, indicting GRP94 specific inhibition in cells. The discovery of **PU-WS13** provided a new tool to investigate the cellular functions of GRP94. **PU-WS13** exposure led to membrane but not cytosolic HER2 reduction in SKBr3 cells, while no same effect was observed in HER2 low-expressing MCF-7 cells. The researchers further demonstrated that GRP94 was important for maintaining the architecture of high-density HER2 formations at the plasma membrane in high HER2-expressing cells. **PU-WS13** treatment induced sub-G1 cell cycle arrest, apoptosis and impaired cell viability in various HER2-overexpressing breast cancer cell lines (Patel et al. 2013). In addition, tumor specific retention effect was also observed for **PU-WS13**, same as the pan-HSP90 inhibitors (Patel et al. 2015). All these results indicated that GRP94 was a promising therapeutic target for HER2-overexpressing breast cancer. The therapeutic effects of **PU-WS13** in multiple myeloma and hepatocellular carcinoma were also observed. In various multiple myeloma cell lines, **PU-WS13** induced both apoptosis and necrosis, and inhibited cell growth. This was believed to be caused by the Wnt-LRP-Survivin pathway blockade effect of **PU-WS13** (Hua et al. 2013). In human HepG2 and PLC hepatocellular carcinoma cell lines, **PU-WS13** treatment exhibited significant growth inhibition effect. In HepG2 cells, **PU-WS13** lowered the levels of total β-catenin and its downstream target cyclin D1, indicating Wnt signaling pathway blockade. **PU-WS13** treated cells also expressed lower levels of hepatocyte growth factor (HGF) and its downstream targets, including p-ERK1/2, p-AKT, and p-STAT3. Further gene expression profile analysis revealed that nine genes involved in cell cycle modulation were down-regulated (Rachidi et al. 2015). All these studies provided proof-of-concept for the anti-cancer effects of GRP94 selective inhibitor **PU-WS13** at cellular level. Further pharmacodynamic evaluation in animal models should be conducted to study the anti-cancer effects of **PU-WS13**.

Another major class of GRP94 selective inhibitors containing resorcinol pharmacophore were developed in Blagg group. Radamide (**RDA**) is a radicicol-geldanamycin chimera that hybrids the resorcinol moiety from radicicol and the quinone moiety form geldanamycin. Further crystal study in Daniel T. Gewirth group showed that **RDA** adopted different conformations to bind with HSP90α and GRP94. In the **RDA**-GRP94 complex, the amide linkage exhibited two orientations. In the cis-amide orientation, the quinone moiety inserted into the GRP94 specific Site 3 and formed van der Waals interactions. In the trans-amide orientation, the quinone moiety was targeted into the solvent area. In the **RDA**-HSP90α complex, the amide linkage only exhibited a trans-amide orientation and the quinone moiety formed tight hydrogen-bonding network with the surrounded residues. These results indicting GRP94 selective inhibitors could be designed based on the cis-amide orientation **RDA** (Duerfeldt et al. 2012; Immormino et al. 2009). In the following study of Blagg group, imidazole was chosen as the bioisoster of cis-amide. Hydrophobic phenyl ring was introduced to form π-interactions with Phe199, Tyr200, and Trp223 in the GRP94 specific Site 3 pocket. These efforts led to **BnIm**, which exhibited 12-fold selectivity for GRP94. **BnIm** treatment inhibited Toll

receptor trafficking and IGF-II secretion in cells. **BnIm** exhibited no cytotoxicity in MCF7, SKBr3, and HEK293 cells even at 100 μM (Duerfeldt et al. 2012). This phenotype was different with the purine-type GRP94 selective inhibitor **PU-WS13**, which exhibited selective anti-proliferative activity against the HER2-overexpressing breast cancer cells. In Gabriela Chiosis group's study, **BnIm** showed little effect on the HER2 expression in SKBr3 cells. The researchers explained that these different phenotypes between **BnIm** and **PU-WS13** might contribute to the different binding modes to GRP94 (Patel et al. 2015). The discovery of **BnIm** provided further insights for the design of GRP94 selective inhibitor, but the low activity and selectivity limited its usage as a probe to study the GRP94 cellular function. Further modification of **BnIm** led to the more potent and selective compound **4** and **KUNG29**. As shown in Fig. 20.6b, crystal structure analysis showed that **4** bound into the Site 3 pocket of GRP94, confirmed the binding mode of this series. **KUNG29** exhibited an IC_{50} value of 0.2 μM for Grp94 and a 41-fold selectivity over HSP90α. In MDA-MB-231 cells, **KUNG29** exhibited potent antimigratory activity without cytotoxicity. Further mechanism study showed that **KUNG29** induced integrin α2 degradation, indicting the antimigratory activity was GRP94 dependent. **KUNG94** was another resorcinol-based GRP94 selective inhibitor. Inspired by the binding mode of **PU-WS13**, hydrophobic moieties were introduced at the 5-position of resorcinol to occupy the GRP94-specific hydrophobic site 2 pocket. SAR study led to **KUNG94** incorporating a 4-fluorobenzyl moiety manifested ~10-fold selectivity for GRP94. The IC_{50} value of **KUNG94** for GRP94 and HSP90α was 8 nM and 77 nM, respectively. In RPMI8226 multiple myeloma cell line, **KUNG94** manifested a GI_{50} value of 1.4 μM. The level of GRP94 specific client LRP6, a Frizzled coreceptor, was reduced after treatment. In addition, the antiapoptotic protein Survivin was reduced, indicting **KUNG94** activated apoptosis through decreasing the Wnt signaling. Considering that **KUNG94** possesses a low selectivity profile and still high inhibition activity to HSP90α, it is difficult to distinguish the cellular effects of GRP94 inhibition and HSP90α inhibition. The selectivity profile of **KUNG94** should be further improved (Khandelwal et al. 2017).

Recently, Blagg group developed an benzamide-containing GRP94 selective inhibitor called **ACO-1** through structure-based design. In this study, aminocyclohexanol-based clinical HSP90 N-terminal inhibitor **SNX2112** was chosen as the rational design template. In order to access the GRP94 specific Site 2 pocket and form additional π interactions with Phe-195, tetrahydroindazolone fragment in **SNX2112** was replaced with a pyrrole, and further SAR study led to **ACO-1**. **ACO-1** manifested an IC_{50} value of 0.44 μM for Grp94 while had no inhibition for HSP90α at 100 μM, displaying over 200-fold selectivity. In PC3-MM2 cells, **ACO-1** treatment led to reduced levels of GRP94 specific clients, including integrin α2, integrin αL, Syne2, VAMP2, and Rab10. These clients are important for the migration process of cancer cells. As significant characteristics during cell migration process, filamentous actin (f-actin) localization and integrin trafficking were inhibited in **ACO-1** treated cells. In further wound healing scratch assay, **ACO-1** potently inhibited the migration of the highly metastatic MDA-MB-231 and

PC3-MM2 cells. These results confirmed the anti-migratory activity of GRP94 selective inhibitors (Mishra et al. 2017).

20.3.2.3 TRAP1 Selective Inhibitors

As TRAP1 involved in multiple processes of cancer development, TRAP1 inhibition has been a promising anti-cancer strategy. Considering that TRAP1 mainly located at mitochondria, mitochondria specific delivery of pan-HSP90 inhibitor is a feasible strategy to inhibit TRAP1. In 2009, Byoung Heon Kang and coworkers developed the first mitochondria-targeted HSP90 inhibitor. Combination of the pan-HSP90 inhibitor **17-AAG** with mitochondrial targeting moieties led to Gamitrinibs (**G-G1**−**G-G4**, **G-TPP**). Gamitrinibs significantly accumulated in the isolated tumor mitochondria and induced immediate loss of inner mitochondrial membrane potential and release of cytochrome c. While the unconjugated **17-AAG** didn't exhibit these properties. Gamitrinibs exhibited potent anti-cancer effects. In lung adenocarcinoma H460 cells, Gamitrinibs treatment significantly induced cell death, mitochondrial apoptosis and decreased colony formation. Unlike **17-AAG**, Gamitrinibs didn't induce degradation of HSP90α clients AKT and Chk1. The HSP70 expression level was also not affected, indicating TRAP1 selective inhibition didn't trigger heat shock response. Gamitrinibs exhibited broad spectrum anti-cancer activity against various cancer cell lines, while exhibited low effects in normal cells, indicting they were selective anti-cancer agents. The anti-cancer effects and safety of Gamitrinibs were further demonstrated in vivo. Gamitrinib (**G-G4**) administration potently inhibited the growth of human leukemia, breast and lung xenograft tumors without significant body weight loss. In the tumors harvested from Gamitrinib-treated animals, extensive apoptosis and release of cytochrome c in the cytosol was observed. In addition, organs of the Gamitrinib-treated animals exhibited similar histological properties compared with the vehicle group, confirmed the safety of Gamitrinib (Kang et al. 2009). Inspired by these preliminary in-vivo anti-cancer effects and safety profile, the researchers then conducted pre-clinical study of gamitrinibs in advanced prostate cancer. In vitro, Gamitrinibs potently inhibited cell viability in prostate cancer cells. In PC3 xenograft tumors, 10 mg/kg i.p. administration of Gamitrinib (**G-TPP**) completely inhibited the tumor growth, while 10 mg/kg **17-AAG** administration exhibited no effect. Meanwhile, no significant weight loss and histological change of organs were observed in the Gamitrinib-treated group. In bone metastatic prostate cancer models, administration of Gamitrinib significantly reduced bone loss compared with the vehicle group (Kang et al. 2010). The anti-cancer effects of Gamitrinib against advanced prostate cancer were further demonstrated in Transgenic Adenocarcinoma of the Mouse Prostate (TRAMP) models. Long-term treatment TRAMP mice with Gamitrinib (**G-G4**) suppressed the formation of localised prostate tumors of neuroendocrine or adenocarcinoma origin, while had no effect on prostatic intraepithelial neoplasia or prostatic inflammation. In addition, the metastasis of prostate cancer to liver and abdominal lymph nodes was also inhibited. No significant animal weight loss or organ toxicity was observed

during treatment (Kang et al. 2011). These results indicated that Gamitrinibs were effective and safe agents for the treatment of advanced prostate cancer. Synergistic anti-cancer activities of Gamitrinib with other agents were observed in various models. In glioblastoma cells, noncytotoxic concentrations of **G-TPP** sensitized tumor cells to TNF-α–related apoptosis-inducing ligand (**TRAIL**). In nude mice carrying intracranial U87-Luc glioblastomas, combination of **TRAIL** and **G-TPP** exhibited potent in-vivo antiglioma activity. Mechanically, **G-TPP** treatment triggered UPR effect. The synergy between **TRAIL** and **G-TPP** was attributed to the UPR-related suppression of NF-κB–dependent gene expression (Siegelin et al. 2011). **G-TPP** also exhibited synergistic anti-cancer effects with doxorubicin. In vitro, combination of **G-TPP** with doxorubicin exhibited enhanced cytotoxicity and apoptotic inducing effect. This synergistic effect was associated with increased expression of pro-apoptotic CHOP and Bim, and the enhanced mitochondrial accumulation of Bim and Bax. In prostate and breast xenograft models, the combination treatment exhibited more potent tumor growth inhibition compared with single treatment with **G-TPP** or doxorubicin. In addition, no aggravating cardiotoxic side effect of doxorubicin was observed during treatment (Park et al. 2014a). **G-TPP** could activate the calcium-mediated UPR in the ER lumen and impair the stress adaptation of cancer cells. Combination treatment with **G-TPP** and ER stressor thapsigargin augmented interorganelle stress signaling, and exhibited synergistic anti-cancer effects. In relapsed prostate cancer xenograft models, **G-TPP** and thapsigargin combination potently inhibited tumor growth (Park et al. 2014b). In general, Gamitrinibs manifested potent in-vitro and in-vivo anti-cancer effects either single used or combined with other agents. They are potential anti-cancer agents and provide proof-of-concept for mitochondrial HSP90 inhibition as novel anti-cancer strategy (Fig. 20.7).

In 2015, Byoung Heon Kang group demonstrated that TRAP1 was the major HSP90 paralogue located in cancer cell mitochondria, with an approximately ten-

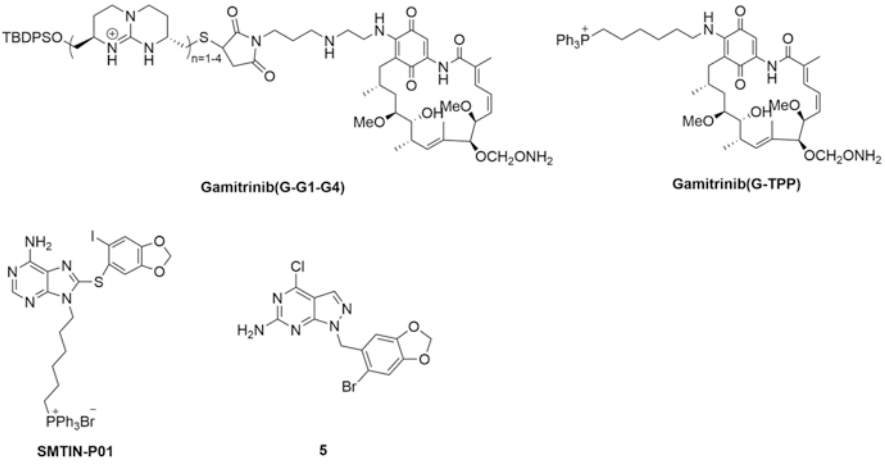

Fig. 20.7 Structures of TRAP1 selective inhibitors

fold higher level than HSP90α/β. In addition, TRAP1 possessed an approximately 32-fold higher ATPase activity. Specific inactivation of TRAP1 alone by siRNA was enough to induce ER UPR in cancer cells. These results indicated that TRAP1 was the predominant target of Gamitrinibs and TRAP1 inhibition was responsible for the potent anti-cancer effects of Gamitrinibs. To design novel TRAP1 selective inhibitor, the researchers resolved the crystal structure of TRAP1 complexed with the pan-HSP90 inhibitor **PU-H71**. Under the guidance of the crystal structure, another mitochondrial TRAP1 inhibitor named **SMTIN-P01** was developed. In **SMTIN-P01**, the solvent-expose isopropyl amine moiety of the **PU-H71** was replaced with the mitochondria-targeting moiety TPP. **SMTIN-P01** exhibited dramatic mitochondria accumulation effect compared with the parent molecule **PU-H71**. In Hela cells, **SMTIN-P01** treatment induced significant mitochondrial membrane depolarization. In addition, the expression levels of HSP90α clients (AKT and Chk1) and HSP70 were not affected, indicating no inhibition on the cytosolic HSP90. In various cancer cell lines, **SMTIN-P01** exhibited more potent cytotoxicity than the parent molecule **PU-H71**. These results confirmed that TRAP1 selective inhibition is an effective anti-cancer strategy (Lee et al. 2015a).

Gamitrinibs and **SMTIN-P01** inhibit TRAP1 via mitochondrial delivery of pan-HSP90 inhibitors, and provide favorable probes to study the function of TRAP1. Alternatively, TRAP1 selective inhibitors with higher affinity to TRAP1 than the cytosolic HSP90α/β may have better applications. Considering the high sequence homologies and the almost superimposable nucleotide-binding sites of the HSP90 four paralogues, development of TRAP1 selective inhibitors is difficult. Recently, the TRAP1 crystal structures complexed with different ligands were resolved, which provided structural guidance for the rational design of TRAP1 selective inhibitors. As shown in Fig. 20.8a, b, some differences were observed in the ligands bound HSP90α and TRAP1. The lid structure (residues 171–201) in TRAP1 was disordered, and

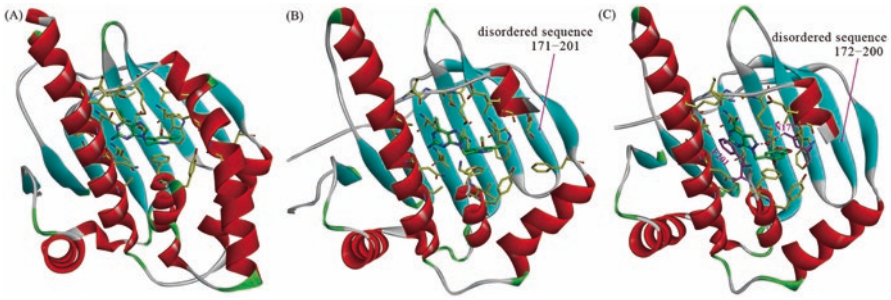

Fig. 20.8 Structural insights of the TRAP1 selective inhibition. (**a**) HSP90α-**BIIB021** complex (PDB ID: 3QDD). (**b**) TRAP1-**BIIB021** complex (PDB ID: 4Z1G), the NTD is intercepted from the $TRAP1_{NM}$. (**c**) TRAP1-5 complex (PDB ID: 5Y3N), the NTD is intercepted from the $TRAP1_{NM}$. The conserved water molecule is shown as red spheres, hydrogen bonds are indicated by magenta dashed lines. Carbon atoms of the compounds are colored in green. N171 and F201 in (**c**) are shown in magenta sticks, other residues are shown in yellow sticks. The active sites of the proteins are surfaced according to the hydrophobic state

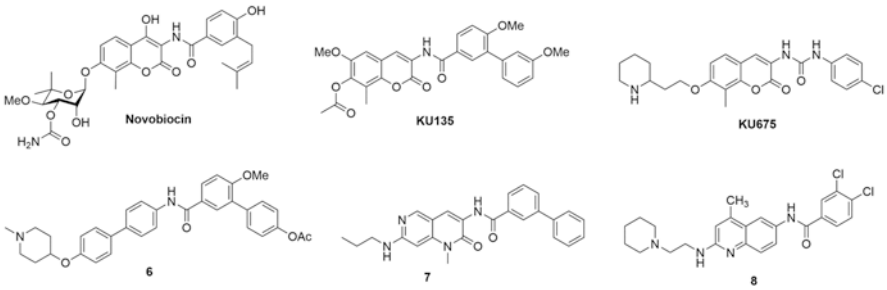

Fig. 20.9 Structures of novobiocin and representative derivatives

residues Asn171 and Gly202 in the two proteins adopted different configurations. These differences indicate compounds that can stabilize the flexible lid structure may manifest TRAP1 selectivity (Lee et al. 2015a; Park et al. 2017). Based on these analyses, Byoung Heon Kang group conducted structure modification focused on **BIIB021** to generate TRAP1 selective inhibitors. The purine scaffold which closed to the disordered lid was changed into pyrazolopyrimidine, then bromopiperonyl was introduced on N-1 position. These efforts led to compound **5**, which exhibited modest TRAP1 selective inhibition (IC_{50} = 79 nM) compared with HSP90α (IC_{50} = 698 nM). Crystal structure analysis confirmed the structural basis for the selectivity. As shown in Figs. 20.8c, compared with the **BIIB021** bound TRAP1, the pyrazolopyrimidine core in **5** formed π-π stacking interaction with the residue Phe201, water-mediated hydrogen bonds were formed between N-2 and Asn171 amide. These additional interactions made great contribution to the TRAP1 selectivity of **5**. In Hela cells, **5** treatment induced loss of mitochondrial membrane potential, overproduction of mitochondrial ROS, elevation of CHOP expression and discharge of cytochrome c, which were all signatures of TRAP1 inhibition. **5** possessed potent cytotoxicity against various cancer cells lines. In PC3 xenograft models, 30 mg/kg daily treatment inhibited tumor growth significantly without toxicity. Both in cancer cells and tumor tissues, **5** treatment had no influence on the HSP70 expression level, indicating no heat shock response was induced (Park et al. 2017). TRAP1 selective inhibitors may overcome the heat shock response effect of pan-HSP90 inhibitors (Fig. 20.9).

20.4 HSP90 C-Terminal Inhibitors

Another ATP-binding pocket is located at the HSP90 CTD. Some inhibitors are reported to occupy this C-terminal ATP-binding pocket and exhibit promising anticancer effects.

20.4.1 Novobiocin and Derivatives

As the first discovered HSP90 C-terminal inhibitor, novobiocin provides a proof-of-concept for HSP90 C-terminal inhibition. In 2000, Neckers and coworkers discovered that novobiocin exhibited HSP90 inhibition activity in a different manner compared with the HSP90 N-terminal inhibitors geldanamycin and radicicol (Marcu et al. 2000b). Further studies demonstrated that novobiocin bound to a second ATP-binding pocket which located at the HSP90 CTD (Marcu et al. 2000a; Soti et al. 2002). In SKBr3 cells, novobiocin treatment reduced $p185^{erbB2}$, mutated P53, and RAF-1 protein levels in a dose-dependent manner (Marcu et al. 2000b). To improve the anti-proliferative effects and simplify the structure of novobiocin, Blagg group conducted extensive SAR study and discovered many derivatives with potent anti-cancer effects. As representative, **KU-135** exhibited dramatically improved anti-proliferative activity against Jurkat T Lymphocytes and melanoma cells compared with novobiocin. **KU135** treatment induced significant mitochondria-mediated apoptosis and G2/M cell cycle arrest in these cells. Moreover, HSP90 client degradations were observed without obvious HSP70 induction (Samadi et al. 2011; Shelton et al. 2009). **KU675** is another novobiocin derivative with potent anti-cancer effects. In both androgen-dependent and -independent prostate cancer cell lines, **KU675** exhibited potent anti-proliferative activity and cytotoxicity. Interestingly, **KU675** exhibited some HSP90α selectivity compared with HSP90β (191 vs 726 μM, K_d in an intrinsic-fluorescence-spectra based binding assay). In prostate cancer cells, **KU675** induced significant degradation of HSP90α specific client proteins (Survivin, B-RAF), but had no obvious effect on the HSP90β specific CXCR4, which confirmed the HSP90α selectivity. In addition, **KU675** manifested Hsc70 binding affinity with a K_d value of 76.3 μM, which associated with the degradation inducing effects of the Hsc70 client proteins Myb and Sp1. **KU675** didn't trigger heat shock response in PC3-MM2 cells, and exhibited a modest down-regulation of HSP (Hsc70 and HSP27) in the LNCap-LN3, LAP C-4, and C4-2 cells (Liu et al. 2015). Compound **6** was a recently developed novobiocin derivative in Blagg group. **6** potently inhibited the proliferation of SKBr3 and MCF-7 cells with IC_{50} of 0.14 and 0.64 μM, respectively (Zhao et al. 2015). David Montoir and coworkers developed another novobiocin derivative **7**, which showed potent anti-proliferative properties in MCF-7 and MDA-MB-468 breast cancer cells (Montoir et al. 2016). Though the above novobiocin derivatives showed potent anti-proliferative activity in cancer cells, the in-vivo anti-tumor efficacy was not evaluated. Recently, our group developed a novobiocin analogue **8** incorporating a 6-acylamino-2-aminoquinoline scaffold. **8** potently inhibited the proliferation of MCF-7 and SKBr3 cells. In MCF-7 cells, **8** inhibited cell migration and induced significant apoptosis. We further evaluated the in-vivo anti-tumor effects of **8** in 4T1 mice breast xenografts. **8** potently inhibited tumor growth and lung metastasis potential without obvious toxicity, indicating **8** was an effective and safe anti-tumor agent

(Jiang et al. 2017). All the above novobiocin derivatives inhibited HSP90 without heat shock response.

20.4.2 Deguelin and Derivatives

Deguelin is a natural rotenoid isolated from several plant species, such as *Mundulea sericea*. In recent years, the potent cancer chemo-preventive and anti-tumor activities of Deguelin against various cancer types have been demonstrated (Lee et al. 2008; Thamilselvan et al. 2011; Udeani et al. 1997). Though some studies indicate that the potent anti-cancer effects of Deguelin is related to the inhibition of several cell signaling pathways, such as PI3K-AKT and GSK-3β/β-catenin, its accurate binding target is still unclear (Chun et al. 2003; Thamilselvan et al. 2011). In 2007, to explore the anti-cancer mechanisms of Deguelin, Oh and coworkers observed that Deguelin could reduce the expression of HIF-1α in a HSP90 inhibition-mediated mechanism. Additionally, Deguelin could induce the degradation of HSP90 clients (CDK4, AKT, eNOS, MEK1/2, and mutant P53) in a time- and dose-dependent manner. ATP-Sepharose assay suggested that Deguelin could bind to HSP90 competitively with ATP, and no activity of Deguelin and its analogues was observed in HSP90 N-terminal inhibitor based fluorescence polarization assay, indicating Deguelin might bind to the HSP90 C-terminal ATP binding pocket (Chang et al. 2012; Oh et al. 2007). In order to elucidate the essential skeleton for the potent HSP90 inhibition activity and discover novel and safe C-terminal inhibitors, Chang and coworkers conducted extensive SAR studies for Deguelin. These efforts led to the discovery of some simplified derivatives with potent anti-proliferative activity (Chang et al. 2012). In the further pre-clinical evaluation, the C-ring truncated **L80** and B, C-ring truncated **SH-1242** exhibited potent anti-tumor effects in various cancer cell lines and xenograft tumor models (Lee et al. 2015b, 2016). It is reported that the potential Parkinsonism-like neurotoxicity of Deguelin may limit its clinical application (Caboni et al. 2004). Compared with Deguelin, **L80** and **SH-1242** displayed significantly reduced cytotoxicity against normal cells. In addition, **SH-1242** didn't produce obvious Parkinsonism-like toxicity in rat brains. These results indicated that **L80** and **SH-1242** were safe anti-cancer agents. In the mechanism study, results of ATP-Sepharose assay and fluorescence-based equilibrium binding assay indicated that the HSP90 inhibition activity of the derivatives was mainly mediated by the direct binding with HSP90 CTD. Docking modeling suggested that the derivatives could bind into the C-terminal ATP-binding pocket and form key interactions with the residues Ser677 and Lys615. Further modification of **L80** and **SH-1242** led to the discovery of the third generation Deguelin derivatives (compound **9** and **10**) (Kim et al. 2015, 2016). The discovery of these novel Deguelin derivatives enriched the structural diversity of HSP90 C-terminal inhibitors and verified the druggable ability of HSP90 C-terminal domain.

20.4.3 Dihydropyrimidinones

Drug design based on the endogenous ligand is an efficient strategy to discover specific inhibitors of the targets. As a successful case, the purine class HSP90 N-terminal inhibitors were designed based on the endogenous ligand ATP (Biamonte et al. 2010). It is reported that the HSP90 CTD nucleotide binding pocket preferred to interact with GTP and UTP (Soti et al. 2003). Therefore, GTP and UTP can serve as the leads to design novel HSP90 C-terminal inhibitors. Inspired by the structural analogy between UTP and the privileged heterocyclic core 3,4-dihydropyrimidin-2-(1H)-one (DHPM), Maria Strocchia and coworkers synthesized several DHPM-based compounds. In Surface Plasmon Resonance (SPR) based binding analysis, seven compounds possessed high binding affinity with the immobilized HSP90α. Compound **11** exhibited moderate cytotoxic effects, which was in line with the SPR affinity. Western-blot analysis showed that compound **11** could induce the HSP90 clients RAF-1 and p-AKT degradation, while the HSP90 and HSP70 levels were not affected. These results verified that compound **11** was an inhibitor of HSP90. Limited proteolysis and oligomerization assays confirmed compound **11** interacting with the C-terminal domain of HSP90α. Further docking analysis showed that compound **11** bound with the region located at the dimerization site interface. Compound **11** was the first reported non-nature-inspired HSP90 C-terminal inhibitor (Strocchia et al. 2015). In order to explore the SARs systematically and discover more potent HSP90 C-terminal inhibitors, researchers conducted further structural modifications and developed the second (**12**) and third generation (**13**) derivatives based on the DHPM core (Terracciano et al. 2016a, b). The two derivatives exhibited improved anti-proliferative activity, especially compound **13**. It inhibited the growth of A375 cancer cells potently with an IC_{50} value of 2.1 ± 0.3 μM. These DHPM-based HSP90 C-terminal inhibitors provided new options for the treatment of cancer and the discovery process provided reference for the design of novel HSP90 C-terminal inhibitors.

20.4.4 EGCG and Derivatives

Epigallocatechin gallate (**EGCG**) is the major polyphenol component in green tea which exhibits broad anti-cancer and chemo-prevention effects. Previously study showed that **EGCG** could inhibit proliferation and induce apoptosis via blocking multiple essential survival pathways in human cancer cells, including JAK/STAT, MAPK, PI3K/AKT, Wnt and Notch (Singh et al. 2011). In 2005, Gasiewicz group first reported that **EGCG** exhibited chemo-preventive effects through directly binding to HSP90 (Palermo et al. 2005). Then they further demonstrated that **EGCG** could inhibit the activity of HSP90 through proteolytic footprinting and immunoprecipitation. Further ATP-agarose pull-down assay declared **EGCG** bound to the

C-terminal ATP binding pocket and interacted with amino acids (538–728) same as novobiocin (Yin et al. 2009). In pancreatic cancer cells, **EGCG** could impair the HSP90 super-chaperone complex and downregulate the HSP90 clients (AKT, Cdk4, RAF-1, Her-2, and pErk) (Li et al. 2009). In addition, **EGCG** inhibited the expression of HSP70 and HSP90 in MCF-7 cells and CT26 xenograft models by inhibiting the expression of the transcription factors HSF1 and HSF2 (Tran et al. 2010). As results, **EGCG** inhibits HSP90 chaperone function with no heat shock response.

To improve the anti-proliferative activity and drug-like properties, Anuj Khandelwal and coworkers conducted structure modification on **EGCG** and illustrated the SARs. The systematical investigation of the four rings and the linker between C- and the D-rings led to discovery of some derivatives with enhanced anti-proliferative activity, such as **14** (IC_{50}, 4 μM in MCF-7 cells). **14** exhibited more than 18-fold improved anti-proliferative activity against MCF-7 cells compared with **EGCG**. It could also induce the HSP90 clients HER2, RAF, and p-AKT degradation in a dose-dependent manner, indicating the potent anti-proliferative activity was HSP90 inhibition dependent (Bhat et al. 2014a). Though the accurate binding modes of **EGCG** and **14** are unclear, they provide novel scaffolds for HSP90 C-terminal inhibitors.

20.4.5 Derrubone and Derivatives

Derrubone is a natural isoflavonoid isolated from the Indian tree *Derris Robusta* (East et al. 1969). It was found to inhibit HSP90 in 2007 by Hadden and coworkers through high-throughput screening based on luciferase refolding inhibition. Derrubone inhibited HSP90-dependent refolding of denatured firefly luciferase with an IC_{50} value of 0.23 ± 0.04 μM. It also exhibited low micro-molar inhibition activity against various cancer cell lines (IC_{50} in MCF-7 and SkBr3 cancer cell lines are 9 and 12 μM, respectively). Meanwhile, the HSP90 clients HER2, RAF-1, AKT and ERα were dose-dependently degraded. Additionally, Derrubone could stabilize the HSP90/CDC37/kinases complex and then prevent the chaperone cycle from progressing (Hadden et al. 2007). Through docking study, Khalid and coworkers predicted that Derrubone might bind to the HSP90 C-terminal ATP-binding pocket and interact with the residues Leu665, Leu666, and Leu694 (Khalid and Paul 2014).

Hastings and coworkers reported the SAR study of Derrubone as HSP90 inhibitors and got three derivatives (**15**–**17**) with improved anti-proliferative activity. Derivative **17** possessed the most potent anti-proliferative activity. Meanwhile, the derivatives could induce the degradation of the clients HER2 and RAF dose-dependently (Hastings et al. 2008). In some extent, further modification can be conducted on Derrubone to improve the HSP90 inhibition and anti-proliferative activity.

20.4.6 Silybin and Derivatives

Silybin, a flavonoid natural product, is the major active constituent in the silymarin that is extracted from milk thistle seeds. In recent years, the anti-cancer effects and chemo-preventive efficacy of Silybin was demonstrated in various cancer types, such as skin, prostate, breast, lung, etc. (Deep and Agarwal 2007; Ting et al. 2013). Encouraged by the promising effects in pre-clinical models, silybin entered clinical trials for safety and pharmacodynamic study (Flaig et al. 2007, 2010; Hoh et al. 2006). The anti-cancer and chemo-preventive mechanisms of silybin have been well studied, including growth inhibition, angiogenesis inhibition, chemo-sensitization, and metastasis inhibition (Desgrosellier and Cheresh 2010). Considering that silybin could block the cell cycle and decrease the Cyclin D1, CDK4 and CDK6 levels (well known HSP90 clients), Zhao and coworkers hypothesized silybin might be a HSP90 inhibitor (Zhao et al. 2011; Zi and Agarwal 1999). The following study showed that silybin could inhibit HSP90-dependent refolding of denatured firefly luciferase (IC_{50}, 0.23 ± 0.04 μM) and induce HSP90 clients (HER2, RAF-1, and AKT) degradation in a dose dependent manner. Riebold and coworkers demonstrated that silybin could bind to HSP90 C-terminal through an ELISA assay. Further NMR spectroscopy analysis suggested that silybin bound to the C-terminal ATP-binding pocket, same as novobiocin (Riebold et al. 2015).

Zhao and coworkers conducted SAR study of silybin. The phenol-removal derivatives **18**, **19**, and **20** exhibited significant improved cytotoxicity against MCF-7 and SKBr3 cancer cell lines. Western blot analysis verified these derivatives induced HSP90 client proteins degradation without heat shock response (Zhao et al. 2011).

20.5 HSP90 Inhibitors Blocking HSP90-CDC37 Protein-Protein Interactions (PPI)

Cochaperones are important components of the HSP90 chaperone machine. They form HSP90-cochaperone complex and regulate the HSP90 chaperone function. Inhibition of the HSP90-cochaperone PPI is a promising strategy to block the HSP90 chaperone function. CDC37 is the kinases specific HSP90 cochaperone. Theoretically, inhibiting the HSP90-CDC37 PPI might specifically block the maturation of the kinase clients, while have no influence on other client proteins. Thus, HSP90-CDC37 PPI inhibitors are speculated to reduce the mechanism related side effects of HSP90 N-terminal inhibitors (Trepel et al. 2010).

Celastrol is the first discovered HSP90-CDC37 PPI inhibitor. In 2008, Duxin Sun lab demonstrated that celastrol could disrupt the HSP90-CDC37 PPI via immunoprecipitation assay. In Panc-1 cells, celastrol treatment induced HSP90 client proteins (CDK4 and AKT) degradation significantly. As results, celastrol inhibited Panc-1 cell growth and induced apoptosis. In Panc-1 xenograft mice, celastrol treatment inhibited tumor growth potently. These studies provided proof-of-concept for

HSP90-CDC37 inhibitors as anti-tumor agents (Kannaiyan et al. 2011). Further study revealed that celastrol covalently bound to CDC37 via a conjugate addition between the Michael reaction acceptor substructure and cysteine residues on CDC37, and then blocked the HSP90-CDC37 interaction (Sreeramulu et al. 2009a). Recently, our lab studied the SARs of celastrol derivatives as HSP90-CDC37 PPI inhibitors and discovered **CEL20**, which exhibited improved HSP90-CDC37 disruption activity and anti-proliferative effects (Jiang et al. 2016a). Some other agents are reported to be HSP90-CDC37 blockers, including Withaferin A, FW-04-806, Apigenin, Sulforaphane and Kongensin A (Wang et al. 2017a). All these agents are natural products incorporating covalent-binding moieties and the accurate HSP90-CDC37 blocking mechanisms are unclear and their further applications are limited. Thus, rational designed HSP90-CDC37 PPI inhibitors with high affinity and clear mechanisms are urgently needed (Figs. 20.10, 20.11, 20.12, 20.13 and 20.14).

The crystal structures of $HSP90_N$-$CDC37_{M/MC}$ complex have been resolved and provides structural insights for the rational design of HSP90-CDC37 PPI inhibitors. As shown in Figs. 20.15, two interaction regions are observed on the $HSP90_N$-$CDC37_M$ interface. The residues on $CDC37_M$ α4 and α5 helix form hydrophobic interactions with the $HSP90_N$ H4 helix. Mutation results suggest that Leu205 is critical for the HSP90-CDC37 PPI. Additionally, the $CDC37_M$ α1 and α2 helix and the connecting loop interact with the H5 helix of $HSP90_N$ (Roe et al. 2004; Sreeramulu et al. 2009b). Recent calculation results in our lab suggest that residues Lys160, His161, Met164, Leu165, Arg166 and Arg167 contributed the most to the binding free energy of the complex, especially the Arg167 (Song et al. 2015).

Peptides derived from the PPI interface are favorable leads for the development of PPI inhibitors. Based on the crystal structures and calculation analysis, our group developed several peptides derived from CDC37 that could block the HSP90-CDC37 PPI. **Pep1** was an 11-peptide directly extracted from CDC37 (sequence 160–170). **Pep1** bound to $HSP90_N$ with K_D value of 6.90 μM and inhibited the HSP90 ATPase with IC_{50} of 3.0 μM. In addition, **Pep1** interfered the HSP90-CDC37

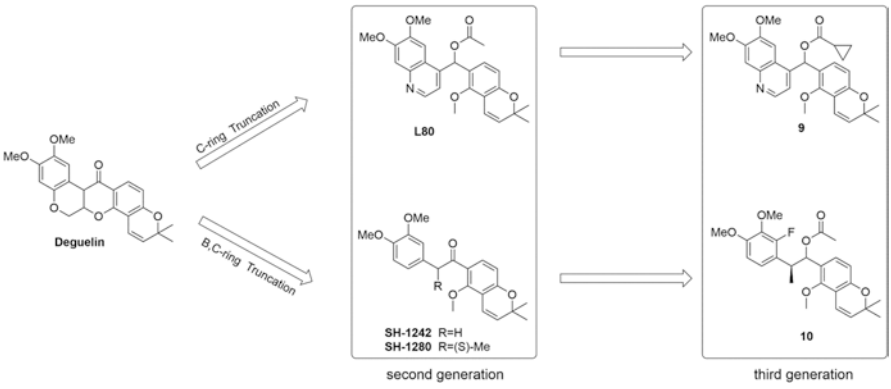

Fig. 20.10 Structures of Deguelin and representative derivatives

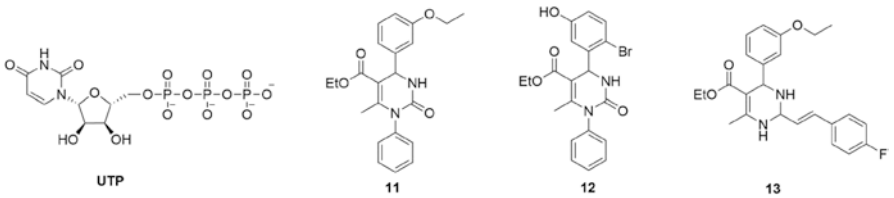

Fig. 20.11 Structures of dihydropyrimidinones as HSP90 C-terminal inhibitors

Fig. 20.12 Structures of EGCG and representative derivative

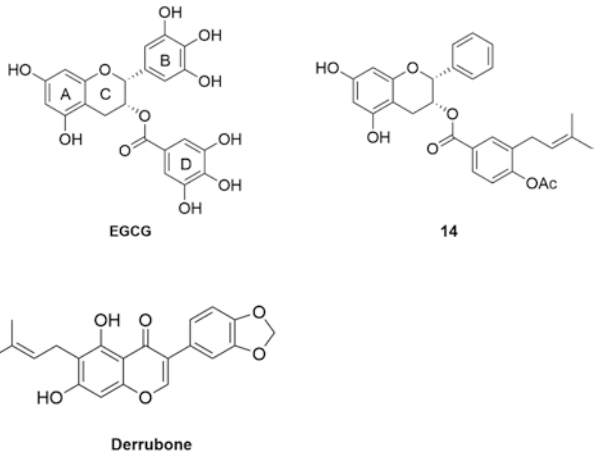

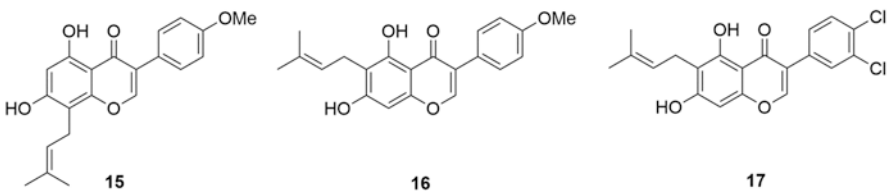

Fig. 20.13 Structures of Derrubone and representative derivatives

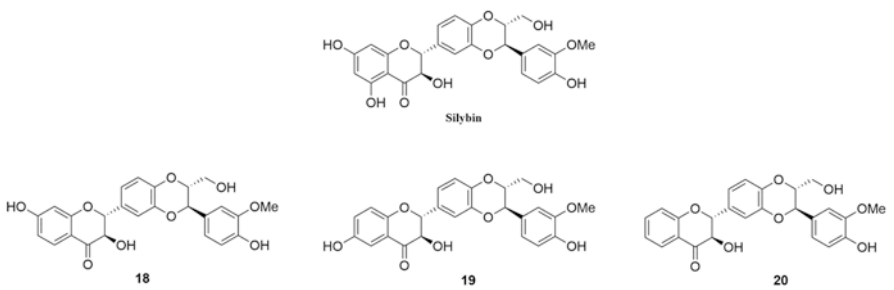

Fig. 20.14 Structures of Silybin and representative derivatives

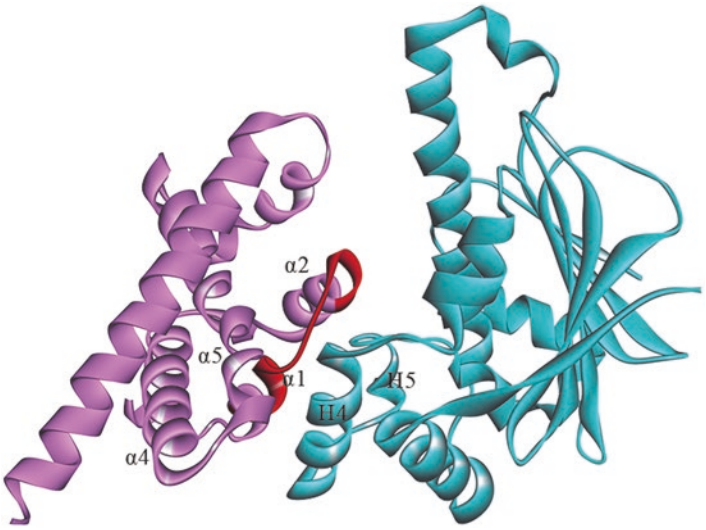

Fig. 20.15 HSP90-CDC37 PPI interface (PDB ID: 2K5B). $HSP90_N$ and $CDC37_M$ are colored in blue and magenta, respectively. Sequence 160–170 on $CDC37_M$ is shown in red, α-helix numbers are indicated

PPI in a biolayer interferometry (BLI) based competitive assay (Wang et al. 2015). Further optimization led to the pentapeptide **Pep5**, which exhibited slightly improved $HSP90_N$ binding affinity with K_D value of 5.99 μM. GST-$HSP90_N$ pull down assay further demonstrated that **Pep5** could block HSP90-CDC37 PPI (Wang et al. 2017b). The discovery of **Pep5** further confirmed that the residues His161, Met164, Leu165, Arg166 and Arg167 on CDC37 were critical for the HSP90-CDC37 PPI. Thus, small molecules disrupting the interactions between these residues and HSP90 can block the HSP90-CDC37 PPI. Based on these results, a pharmacophore model was generated and used for virtual screening to discover HSP90-CDC37 PPI inhibitors. Fortunately, we discovered compound **VS-8** exhibited moderate HSP90-CDC37 PPI inhibition activity with IC_{50} value of 76.85 μM in Homogeneous Time-Resolved Fluorescence (HTRF) assay. Further optimization of **VS-8** led to compound **21**, which exhibited threefold improved activity with IC_{50} value of 27.40 μM. Compound **21** bound to HSP90 with K_D value of 40.4 μM. In GST-pull down assay, **21** blocked HSP90-CDC37 interaction in a dose dependently manner. Moreover, **21** possessed moderated anti-proliferative activity in cancer cells and induced HSP90 kinase clients AKT and CDK4 degradation (Wang et al. 2017b). As the first reported non-natural small molecule HSP90-CDC37 PPI inhibitor, **21** can serve as a probe to study the HSP90-CDC37 PPI (Fig. 20.16).

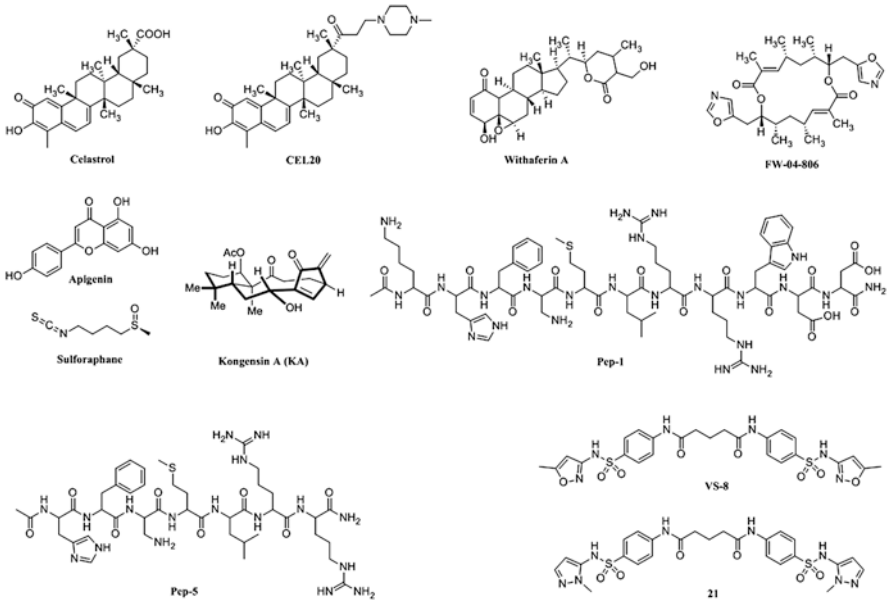

Fig. 20.16 Structures of HSP90-CDC37 PPI inhibitors

20.6 Conclusions

HSP90 isoforms are involved in multiple processes of cancer development, and HSP90 inhibition has been a promising anti-cancer strategy. Till now, HSP90 inhibitors with different mechanisms have been developed. Many pan-HSP90 N-terminal inhibitors have entered clinical trials. Despite the potent pre-clinical anti-cancer effects, these inhibitors exhibit disappointing clinical efficacy. In addition, many serious adverse effects are occurred during the treatment, such as the ocular toxicity. The adverse effects may limit the clinical dosage, which is a possible reason for the poor clinical efficacy. Heat shock response triggered by the pan-HSP90 inhibitors may be another reason. Thus, inhibitors with reduced adverse effects and no heat shock response may bring breakthrough for the HSP90 inhibitor development. HSP90 four isoforms have different functions and client protein profiles, so isoform selective inhibitors may have reduced adverse effects. **TAS-116** is a HSP90α/β selective inhibitor which has entered clinical trials, and moderate clinical anti-cancer effects are observed in patients with advanced solid tumors. For further clinical studies, **TAS-116** should be evaluated in more cancer types to find the most sensitive patient populations. Moreover, the heat shock response effect should be a concern of **TAS-116**, which may neutralize the anti-cancer effects. GRP94 selective inhibition and TRAP1 selective inhibition don't trigger heat shock response, may be more promising. GRP94 inhibitor **PU-WS13** exhibited favorable anti-proliferative

activity in HER2-overexpressing breast cancer cells and multiple myeloma cells. Additionally, some GRP94 inhibitors possess anti-migratory potential. The anti-cancer effects of GRP94 selective inhibitors should be further evaluated in pre-clinical study. Studies of Byoung Heon Kang and coworkers demonstrate TRAP-1 selective inhibition is a promising anti-cancer strategy. Though Gamitrinibs and **SMTIN-P01** possess potent anti-cancer effects, their clinical application may be limited. Compound **5** exhibits moderated TRAP1 selectivity compared with cytosolic HSP90, the selectivity profile should be improved in further modification. HSP90 C-terminal inhibition doesn't induce heat shock response, is another promising HSP90 inhibition strategy. Most reported HSP90 C-terminal inhibitors are natural product analogues, and their accurate binding modes are still unclear. In future study, more efforts should be done to reveal the binding modes of the C-terminal inhibitors. This will promote the development of HSP90 C-terminal inhibitors. HSP90-cochaperone PPI inhibition is an attractive strategy to inhibit the HSP90 chaperone function. CDC37 is a cochaperone which specifically regulate the maturation of kinase client proteins. Theoretically, HSP90-cochaperone PPI inhibition will only block the maturation of kinase clients and have no influence on other client proteins. Thus, HSP90-CDC37 PPI inhibitors can reduce the mechanism related adverse effects of the pan-HSP90 inhibitors. All previously reported HSP90-CDC37 PPI inhibitors incorporate a covalent-binding moiety and the HSP90-CDC37 PPI inhibition activity is covalent-binding based. Thus, rational designed HSP90-CDC37 PPI inhibitors are urgently needed. Our group have explored the hot-spots of the HSP90-CDC37 interface and discovered compound **21** as the first small-molecule HSP90-CDC37 inhibitor. **21** manifests moderate HSP90-CDC37 PPI blocking activity, and the activity should be further improved. Moreover, the anti-cancer effects of HSP90-CDC37 PPI inhibitors should be further studied. In general, HSP90 chaperone function inhibition is a promising anti-cancer strategy, but there is still a long way to go.

Acknowledgements This work is supported by Projects 81872737 and 81773639 of the National Natural Science Foundation of China; 2632018ZD15 of the Key Program of China Pharmaceutical University; 2017ZX0-9302003, and 2018ZX09711002-003-006 of the National Major Science and Technology Project of China (Innovation and Development of New Drugs).

References

Agorreta J, Hu J, Liu D et al (2014) TRAP1 regulates proliferation, mitochondrial function, and has prognostic significance in NSCLC. Mol Cancer Res 12(5):660–669

Barrott JJ, Haystead TA (2013) Hsp90, an unlikely ally in the war on cancer. FEBS J 280(6):1381–1396

Barton ER, Park S, James JK et al (2012) Deletion of muscle GRP94 impairs both muscle and body growth by inhibiting local IGF production. FASEB J 26(9):3691–3702

Bhat R, Adam AT, Lee JJ, Gasiewicz TA, Henry EC, Rotella DP (2014a) Towards the discovery of drug-like epigallocatechin gallate analogs as Hsp90 inhibitors. Bioorg Med Chem Lett 24(10):2263–2266

Bhat R, Tummalapalli SR, Rotella DP (2014b) Progress in the discovery and development of heat shock protein 90 (Hsp90) inhibitors. J Med Chem 57(21):8718–8728
Biamonte MA, Van de Water R, Arndt JW, Scannevin RH, Perret D, Lee W-C (2010) Heat shock protein 90: inhibitors in clinical trials. J Med Chem 53(1):3–17
Brahmkhatri VP, Prasanna C, Atreya HS (2015) Insulin-like growth factor system in cancer: novel targeted therapies. Biomed Res Int 2015:538019–538042
Caboni P, Sherer TB, Zhang N et al (2004) Rotenone, deguelin, their metabolites, and the rat model of Parkinson's disease. Chem Res Toxicol 17(11):1540–1548
Calderwood SK (2013) Molecular cochaperones: tumor growth and cancer treatment. Scientifica (Cairo) 2013:217513–217525
Chang DJ, An H, Kim KS et al (2012) Design, synthesis, and biological evaluation of novel deguelin-based heat shock protein 90 (HSP90) inhibitors targeting proliferation and angiogenesis. J Med Chem 55(24):10863–10884
Chen Y, Chen C, Ma C, Sun S, Zhang J, Sun Y (2015) Expression of heat-shock protein gp96 in gallbladder cancer and its prognostic clinical significance. Int J Clin Exp Pathol 8(2):1946–1953
Chhabra S, Jain S, Wallace C, Hong F, Liu B (2015) High expression of endoplasmic reticulum chaperone grp94 is a novel molecular hallmark of malignant plasma cells in multiple myeloma. J Hematol Oncol 8:77–85
Chun KH, Kosmeder JW 2nd, Sun S et al (2003) Effects of deguelin on the phosphatidylinositol 3-kinase/Akt pathway and apoptosis in premalignant human bronchial epithelial cells. J Natl Cancer Inst 95(4):291–302
Costantino E, Maddalena F, Calise S et al (2009) TRAP1, a novel mitochondrial chaperone responsible for multi-drug resistance and protection from apoptotis in human colorectal carcinoma cells. Cancer Lett 279(1):39–46
Deep G, Agarwal R (2007) Chemopreventive efficacy of silymarin in skin and prostate cancer. Integr Cancer Ther 6(2):130–145
Dejeans N, Glorieux C, Guenin S et al (2012) Overexpression of GRP94 in breast cancer cells resistant to oxidative stress promotes high levels of cancer cell proliferation and migration: implications for tumor recurrence. Free Radic Biol Med 52(6):993–1002
Desgrosellier JS, Cheresh DA (2010) Integrins in cancer: biological implications and therapeutic opportunities. Nat Rev Cancer 10(1):9–22
Duerfeldt AS, Peterson LB, Maynard JC et al (2012) Development of a Grp94 inhibitor. J Am Chem Soc 134(23):9796–9804
East AJ, Ollis WD, Wheeler RE (1969) Natural occurrence of 3-aryl-4-hydroxycoumarins. Part I. Phytochemical examination of Derris robusta (Roxb.) Benth. J Chem Soc C 3(3):365–374
Ernst JT, Liu M, Zuccola H et al (2014a) Correlation between chemotype-dependent binding conformations of HSP90alpha/beta and isoform selectivity-implications for the structure-based design of HSP90alpha/beta selective inhibitors for treating neurodegenerative diseases. Bioorg Med Chem Lett 24(1):204–208
Ernst JT, Neubert T, Liu M et al (2014b) Identification of novel HSP90alpha/beta isoform selective inhibitors using structure-based drug design. Demonstration of potential utility in treating CNS disorders such as Huntington's disease. J Med Chem 57(8):3382–3400
Flaig TW, Gustafson DL, Su LJ et al (2007) A phase I and pharmacokinetic study of silybin-phytosome in prostate cancer patients. Investig New Drugs 25(2):139–146
Flaig TW, Glode M, Gustafson D et al (2010) A study of high-dose oral silybin-phytosome followed by prostatectomy in patients with localized prostate cancer. Prostate 70(8):848–855
Garcia-Carbonero R, Carnero A, Paz-Ares L (2013) Inhibition of HSP90 molecular chaperones: moving into the clinic. Lancet Oncol 14(9):E358–E369
Gewirth DT (2016) Paralog specific Hsp90 inhibitors – a brief history and a bright future. Curr Top Med Chem 16(25):2779–2791
Hadden MK, Galam L, Gestwicki JE, Matts RL, Blagg BS (2007) Derrubone, an inhibitor of the Hsp90 protein folding machinery. J Nat Prod 70(12):2014–2018
Hastings JM, Hadden MK, Blagg BS (2008) Synthesis and evaluation of derrubone and select analogues. J Org Chem 73(2):369–373

Hoh C, Boocock D, Marczylo T et al (2006) Pilot study of oral silibinin, a putative chemopreventive agent, in colorectal cancer patients: silibinin levels in plasma, colorectum, and liver and their pharmacodynamic consequences. Clin Cancer Res 12(9):2944–2950

Hong F, Liu B, Chiosis G, Gewirth DT, Li Z (2013) alpha7 helix region of alphaI domain is crucial for integrin binding to endoplasmic reticulum chaperone gp96: a potential therapeutic target for cancer metastasis. J Biol Chem 288(25):18243–18248

Hua Y, White-Gilbertson S, Kellner J et al (2013) Molecular chaperone gp96 is a novel therapeutic target of multiple myeloma. Clin Cancer Res 19(22):6242–6251

Immormino RM, Metzger LE t, Reardon PN, Dollins DE, Blagg BS, Gewirth DT (2009) Different poses for ligand and chaperone in inhibitor-bound Hsp90 and GRP94: implications for paralog-specific drug design. J Mol Biol 388(5):1033–1042

Jiang F, Wang HJ, Bao QC et al (2016a) Optimization and biological evaluation of celastrol derivatives as Hsp90-Cdc37 interaction disruptors with improved druglike properties. Bioorg Med Chem 24(21):5431–5439

Jiang F, Wang HJ, Jin YH et al (2016b) Novel tetrahydropyrido[4,3-d]pyrimidines as potent inhibitors of chaperone heat shock protein 90. J Med Chem 59(23):10498–10519

Jiang F, Guo AP, Xu JC et al (2017) Identification and optimization of novel 6-acylamino-2-aminoquinolines as potent Hsp90 C-terminal inhibitors. Eur J Med Chem 141:1–14

Kaiser M, Lamottke B, Mieth M et al (2010) Synergistic action of the novel HSP90 inhibitor NVP-AUY922 with histone deacetylase inhibitors, melphalan, or doxorubicin in multiple myeloma. Eur J Haematol 84(4):337–344

Kang BH, Plescia J, Song HY et al (2009) Combinatorial drug design targeting multiple cancer signaling networks controlled by mitochondrial Hsp90. J Clin Invest 119(3):454–464

Kang BH, Siegelin MD, Plescia J et al (2010) Preclinical characterization of mitochondria-targeted small molecule hsp90 inhibitors, gamitrinibs, in advanced prostate cancer. Clin Cancer Res 16(19):4779–4788

Kang BH, Tavecchio M, Goel HL et al (2011) Targeted inhibition of mitochondrial Hsp90 suppresses localised and metastatic prostate cancer growth in a genetic mouse model of disease. Br J Cancer 104(4):629–634

Kannaiyan R, Shanmugam MK, Sethi G (2011) Molecular targets of celastrol derived from Thunder of God Vine: potential role in the treatment of inflammatory disorders and cancer. Cancer Lett 303(1):9–20

Khalid S, Paul S (2014) Identifying a C-terminal ATP binding sites-based novel Hsp90-Inhibitor in silico: a plausible therapeutic approach in Alzheimer's disease. Med Hypotheses 83(1):39–46

Khandelwal A, Crowley VM, Blagg BSJ (2017) Resorcinol-based Grp94-selective inhibitors. ACS Med Chem Lett 8(10):1013–1018

Kim HS, Hong M, Lee SC et al (2015) Ring-truncated deguelin derivatives as potent Hypoxia Inducible Factor-1alpha (HIF-1alpha) inhibitors. Eur J Med Chem 104:157–164

Kim HS, Hong M, Ann J et al (2016) Synthesis and biological evaluation of C-ring truncated deguelin derivatives as heat shock protein 90 (HSP90) inhibitors. Bioorg Med Chem 24(22):6082–6093

King ER, Wong KK (2012) Insulin-like growth factor: current concepts and new developments in cancer therapy. Recent Pat Anticancer Drug Discov 7(1):14–30

Kurokawa Y, Doi T, Sawaki A, et al. (2017) Phase II study of TAS-116, an oral inhibitor of heat shock protein 90 (HSP90), in metastatic or unresectable gastrointestinal stromal tumor refractory to imatinib, sunitinib and regorafenib. 41st Eur Soc Med Oncol (ESMO) Congr (September 8–12, Madrid) 2017, Abst 1479PD

Landriscina M, Amoroso MR, Piscazzi A, Esposito F (2010) Heat shock proteins, cell survival and drug resistance: the mitochondrial chaperone TRAP1, a potential novel target for ovarian cancer therapy. Gynecol Oncol 117(2):177–182

Leav I, Plescia J, Goel HL et al (2010) Cytoprotective mitochondrial chaperone TRAP-1 as a novel molecular target in localized and metastatic prostate cancer. Am J Pathol 176(1):393–401

Lee JH, Lee DH, Lee HS, Choi JS, Kim KW, Hong SS (2008) Deguelin inhibits human hepatocellular carcinoma by antiangiogenesis and apoptosis. Oncol Rep 20(1):129–134

Lee C, Park HK, Jeong H et al (2015a) Development of a mitochondria-targeted Hsp90 inhibitor based on the crystal structures of human TRAP1. J Am Chem Soc 137(13):4358–4367

Lee SC, Min HY, Choi H et al (2015b) Synthesis and evaluation of a novel deguelin derivative, L80, which disrupts ATP binding to the C-terminal domain of heat shock protein 90. Mol Pharmacol 88(2):245–255

Lee SC, Min HY, Choi H et al (2016) Deguelin analogue SH-1242 inhibits Hsp90 activity and exerts potent anticancer efficacy with limited neurotoxicity. Cancer Res 76(3):686–699

Li Y, Zhang T, Jiang Y, Lee H-F, Schwartz SJ, Sun D (2009) (−)-Epigallocatechin-3-gallate inhibits Hsp90 function by impairing Hsp90 association with co-chaperones in pancreatic cancer cell line Mia Paca-2. Mol Pharm 6(4):1152–1159

Li X, Sun L, Hou J et al (2015a) Cell membrane gp96 facilitates HER2 dimerization and serves as a novel target in breast cancer. Int J Cancer 137(3):512–524

Li X, Wang B, Liu W, Gui M, Peng Z, Meng S (2015b) Blockage of conformational changes of heat shock protein gp96 on cell membrane by an alpha-helix peptide inhibits HER2 dimerization and signaling in breast cancer. PLoS One 10(4):e0124647–e0124658

Liu B, Staron M, Hong F et al (2013) Essential roles of grp94 in gut homeostasis via chaperoning canonical Wnt pathway. Proc Natl Acad Sci U S A 110(17):6877–6882

Liu W, Vielhauer GA, Holzbeierlein JM et al (2015) KU675, a concomitant heat-shock protein inhibitor of Hsp90 and Hsc70 that manifests isoform selectivity for Hsp90 a in prostate cancer cells. Mol Pharmacol 88(1):121–130

Maddalena F, Sisinni L, Lettini G et al (2013) Resistance to paclitxel in breast carcinoma cells requires a quality control of mitochondrial antiapoptotic proteins by TRAP1. Mol Oncol 7(5):895–906

Marcu MG, Chadli A, Bouhouche I, Catelli M, Neckers LM (2000a) The heat shock protein 90 antagonist novobiocin interacts with a previously unrecognized ATP-binding domain in the carboxyl terminus of the chaperone. J Biol Chem 275(47):37181–37186

Marcu MG, Schulte TW, Neckers L (2000b) Novobiocin and related coumarins and depletion of heat shock protein 90-dependent signaling proteins. J Natl Cancer Inst 92(3):242–248

Marzec M, Hawkes CP, Eletto D et al (2016) A human variant of glucose-regulated protein 94 that inefficiently supports IGF production. Endocrinology 157(5):1914–1928

Mishra SJ, Ghosh S, Stothert AR, Dickey CA, Blagg BS (2017) Transformation of the non-selective aminocyclohexanol-based Hsp90 inhibitor into a Grp94-seletive scaffold. ACS Chem Biol 12(1):244–253

Miyata Y, Nakamoto H, Neckers L (2013) The therapeutic target Hsp90 and cancer hallmarks. Curr Pharm Des 19(3):347–365

Montoir D, Barillé-Nion S, Tonnerre A, Juin P, Duflos M, Bazin M-A (2016) Novel 1,6-naphthyridin-2(1H)-ones as potential anticancer agents targeting Hsp90. Eur J Med Chem 119:17–33

Oh SH, Woo JK, Yazici YD et al (2007) Structural basis for depletion of heat shock protein 90 client proteins by deguelin. J Natl Cancer Inst 99(12):949–961

Ohkubo S, Muraoka H, Hashimoto A et al (2012) Evolution of highly selective HSP90α/β Inhibitors with unique binding mode. Eur J Cancer 48:89–89

Ohkubo S, Kodama Y, Muraoka H et al (2015) TAS-116, a highly selective inhibitor of heat shock protein 90alpha and beta, demonstrates potent antitumor activity and minimal ocular toxicity in preclinical models. Mol Cancer Ther 14(1):14–22

Ostrovsky O, Ahmed NT, Argon Y (2009) The chaperone activity of GRP94 toward insulin-like growth factor II is necessary for the stress response to serum deprivation. Mol Biol Cell 20(6):1855–1864

Palermo CM, Westlake CA, Gasiewicz TA (2005) Epigallocatechin gallate inhibits aryl hydrocarbon receptor gene transcription through an indirect mechanism involving binding to a 90 kDa heat shock protein. Biochemistry 44(13):5041–5052

Park H-K, Lee J-E, Lim J et al (2014a) Combination treatment with doxorubicin and gamitrinib synergistically augments anticancer activity through enhanced activation of Bim. BMC Cancer 14:431–431

Park H-K, Lee J-E, Lim J, Kang BH (2014b) Mitochondrial Hsp90s suppress calcium-mediated stress signals propagating from mitochondria to the ER in cancer cells. Mol Cancer 13:148–148
Park HK, Jeong H, Ko E et al (2017) Paralog specificity determines subcellular distribution, action mechanism, and anticancer activity of TRAP1 inhibitors. J Med Chem 60(17):7569–7578
Patel PD, Yan P, Seidler PM et al (2013) Paralog-selective Hsp90 inhibitors define tumor-specific regulation of HER2. Nat Chem Biol 9(11):677–684
Patel HJ, Patel PD, Ochiana SO et al (2015) Structure-activity relationship in a purine-scaffold compound series with selectivity for the endoplasmic reticulum Hsp90 paralog Grp94. J Med Chem 58(9):3922–3943
Patterson J, Palombella VJ, Fritz C, Normant E (2008) IPI-504, a novel and soluble HSP-90 inhibitor, blocks the unfolded protein response in multiple myeloma cells. Cancer Chemother Pharmacol 61(6):923–932
Rachidi S, Sun S, Wu BX et al (2015) Endoplasmic reticulum heat shock protein gp96 maintains liver homeostasis and promotes hepatocellular carcinogenesis. J Hepatol 62(4):879–888
Richardson PG, Badros AZ, Jagannath S et al (2010a) Tanespimycin with bortezomib: activity in relapsed/refractory patients with multiple myeloma. Br J Haematol 150(4):428–437
Richardson PG, Chanan-Khan AA, Alsina M et al (2010b) Tanespimycin monotherapy in relapsed multiple myeloma: results of a phase 1 dose-escalation study. Br J Haematol 150(4):438–445
Richardson PG, Chanan-Khan AA, Lonial S et al (2011) Tanespimycin and bortezomib combination treatment in patients with relapsed or relapsed and refractory multiple myeloma: results of a phase 1/2 study. Br J Haematol 153(6):729–740
Riebold M, Kozany C, Freiburger L et al (2015) A C-terminal HSP90 inhibitor restores glucocorticoid sensitivity and relieves a mouse allograft model of Cushing disease. Nat Med 21(3):276–280
Roe SM, Ali MM, Meyer P et al (2004) The mechanism of Hsp90 regulation by the protein kinase-specific cochaperone p50(cdc37). Cell 116(1):87–98
Rosser MF, Nicchitta CV (2000) Ligand interactions in the adenosine nucleotide-binding domain of the Hsp90 chaperone, GRP94. I. Evidence for allosteric regulation of ligand binding. J Biol Chem 275(30):22798–22805
Samadi AK, Zhang X, Mukerji R, Donnelly AC, Blagg BS, Cohen MS (2011) A novel C-terminal HSP90 inhibitor KU135 induces apoptosis and cell cycle arrest in melanoma cells. Cancer Lett 312(2):158–167
Sciacovelli M, Guzzo G, Morello V et al (2013) The mitochondrial chaperone TRAP1 promotes neoplastic growth by inhibiting succinate dehydrogenase. Cell Metab 17(6):988–999
Shelton SN, Shawgo ME, Matthews SB et al (2009) KU135, a novel novobiocin-derived C-terminal inhibitor of the 90-kDa heat shock protein, exerts potent antiproliferative effects in human leukemic cells. Mol Pharmacol 76(6):1314–1322
Shimomura A, Horiike A, Tambo Y et al (2015) First-in-human phase I dose escalation study of TAS-116, a novel, orally active HSP90α and HSP90β selective inhibitor, in patients with advanced solid tumors. Mol Cancer Ther 14(12 Supplement 2):B87
Siegelin MD, Dohi T, Raskett CM et al (2011) Exploiting the mitochondrial unfolded protein response for cancer therapy in mice and human cells. J Clin Invest 121(4):1349–1360
Singh BN, Shankar S, Srivastava RK (2011) Green tea catechin, epigallocatechin-3-gallate (EGCG): mechanisms, perspectives and clinical applications. Biochem Pharmacol 82(12):1807–1821
Sisinni L, Maddalena F, Lettini G et al (2014) TRAP1 role in endoplasmic reticulum stress protection favors resistance to anthracyclins in breast carcinoma cells. Int J Oncol 44(2):573–582
Song X, Zhao Z, Qi X et al (2015) Identification of epipolythiodioxopiperazines HDN-1 and chaetocin as novel inhibitor of heat shock protein 90. Oncotarget 6(7):5263–5274
Soti C, Racz A, Csermely P (2002) A nucleotide-dependent molecular switch controls ATP binding at the C-terminal domain of Hsp90. N-terminal nucleotide binding unmasks a C-terminal binding pocket. J Biol Chem 277(9):7066–7075
Soti C, Vermes A, Haystead TAJ, Csermely P (2003) Comparative analysis of the ATP-binding sites of Hsp90 by nucleotide affinity cleavage: a distinct nucleotide specificity of the C-terminal ATP-binding site. Eur J Biochem 270(11):2421–2428

Sreeramulu S, Gande SL, Gobel M, Schwalbe H (2009a) Molecular mechanism of inhibition of the human protein complex Hsp90-Cdc37, a kinome chaperone-cochaperone, by triterpene celastrol. Angew Chem Int Ed Engl 48(32):5853–5855

Sreeramulu S, Jonker HR, Langer T, Richter C, Lancaster CR, Schwalbe H (2009b) The human Cdc37.Hsp90 complex studied by heteronuclear NMR spectroscopy. J Biol Chem 284(6):3885–3896

Strocchia M, Terracciano S, Chini MG et al (2015) Targeting the Hsp90 C-terminal domain by the chemically accessible dihydropyrimidinone scaffold. Chem Commun (Camb) 51(18):3850–3853

Stuhmer T, Zollinger A, Siegmund D et al (2008) Signalling profile and antitumour activity of the novel Hsp90 inhibitor NVP-AUY922 in multiple myeloma. Leukemia 22(8):1604–1612

Suzuki R, Hideshima T, Mimura N et al (2015a) Anti-tumor activities of selective HSP90alpha/beta inhibitor, TAS-116, in combination with bortezomib in multiple myeloma. Leukemia 29(2):510–514

Suzuki R, Kikuchi S, Harada T et al (2015b) Combination of a selective HSP90α/β inhibitor and a RAS-RAF-MEK-ERK signaling pathway inhibitor triggers synergistic cytotoxicity in multiple myeloma cells. PLoS One 10(12):e0143847–e0143866

Takanami I (2005) Increased expression of integrin-linked kinase is associated with shorter survival in non-small cell lung cancer. BMC Cancer 5:1–7

Terracciano S, Chini MG, Vaccaro MC et al (2016a) Identification of the key structural elements of a dihydropyrimidinone core driving toward more potent Hsp90 C-terminal inhibitors. Chem Commun (Camb) 52(87):12857–12860

Terracciano S, Foglia A, Chini MG et al (2016b) New dihydropyrimidin-2(1H)-one based Hsp90 C-terminal inhibitors. RSC Adv 6(85):82330–82340

Thamilselvan V, Menon M, Thamilselvan S (2011) Anticancer efficacy of deguelin in human prostate cancer cells targeting glycogen synthase kinase-3 beta/beta-catenin pathway. Int J Cancer 129(12):2916–2927

Tian X, Ma P, Sui CG et al (2014) Suppression of tumor necrosis factor receptor-associated protein 1 expression induces inhibition of cell proliferation and tumor growth in human esophageal cancer cells. FEBS J 281(12):2805–2819

Ting H, Deep G, Agarwal R (2013) Molecular mechanisms of silibinin-mediated cancer chemoprevention with major emphasis on prostate cancer. AAPS J 15(3):707–716

Tran PL, Kim S-A, Choi HS, Yoon J-H, Ahn S-G (2010) Epigallocatechin-3-gallate suppresses the expression of HSP70 and HSP90 and exhibits anti-tumor activity in vitro and in vivo. BMC Cancer 10(1):276–284

Trepel J, Mollapour M, Giaccone G, Neckers L (2010) Targeting the dynamic HSP90 complex in cancer. Nat Rev Cancer 10(8):537–549

Udeani GO, Gerhauser C, Thomas CF et al (1997) Cancer chemopreventive activity mediated by deguelin, a naturally occurring rotenoid. Cancer Res 57(16):3424–3428

Verma S, Goyal S, Jamal S, Singh A, Grover A (2016) Hsp90: friends, clients and natural foes. Biochimie 127:227–240

Wanderling S, Simen BB, Ostrovsky O et al (2007) GRP94 is essential for mesoderm induction and muscle development because it regulates insulin-like growth factor secretion. Mol Biol Cell 18(10):3764–3775

Wang L, Bao Q-C, Xu X-L et al (2015) Discovery and identification of Cdc37-derived peptides targeting the Hsp90–Cdc37 protein–protein interaction. RSC Adv 5(116):96138–96145

Wang L, Li L, Gu K, Xu XL, Sun Y, You QD (2017a) Targeting Hsp90-Cdc37: a promising therapeutic strategy by inhibiting Hsp90 chaperone function. Curr Drug Targets 18(13):1572–1585

Wang L, Li L, Zhou ZH, Jiang ZY, You QD, Xu XL (2017b) Structure-based virtual screening and optimization of modulators targeting Hsp90-Cdc37 interaction. Eur J Med Chem 136:63–73

Yanagitani N, Horiike A, Kitazono S, et al. (2017) First-in-human phase I study of an oral HSP90 inhibitor, TAS-116, in advanced solid tumors. 53rd Ann Meet Am Soc Clin Oncol (ASCO) (June 2–6, Chicago) 2017, Abst 2546

Yin Z, Henry EC, Gasiewicz TA (2009) (-)-Epigallocatechin-3-gallate is a novel HSP90 inhibitor. Biochemistry 48(2):336–345

Zhao H, Brandt GE, Galam L, Matts RL, Blagg BSJ (2011) Identification and initial SAR of silybin: an Hsp90 inhibitor. Bioorg Med Chem Lett 21(9):2659–2664

Zhao H, Garg G, Zhao J et al (2015) Design, synthesis and biological evaluation of biphenylamide derivatives as Hsp90 C-terminal inhibitors. Eur J Med Chem 89:442–466

Zi X, Agarwal R (1999) Silibinin decreases prostate-specific antigen with cell growth inhibition via G1 arrest, leading to differentiation of prostate carcinoma cells: implications for prostate cancer intervention. Proc Natl Acad Sci U S A 96(13):7490–7495